IPPT PAN
• Institute of Fundamental Technological Research •
• Polish Academy of Sciences •
• Warsaw • Poland •

LECTURE NOTES 7

Theoretical Foundations of Biomechanics

Peter Niederer

Institute of Biomedical Engineering
University of Zurich and Swiss Federal Institute
of Technology, Zurich, Switzerland

abiomed

Centre of Excellence for
Applied Biomedical Modelling and Diagnostics

WARSAW 2005

ABIOMED LECTURE NOTES

ISSN 1733-0874

Skład: Maciej Stańczyk
Papier offset. kl. III, 70 g, B1
Oddano do druku: XII 2005; druk ukończono: XII 2005
Druk i oprawa: Drukarnia Braci Grodzickich, Piaseczno, ul. Geodetów 47a

Contents

Preface

This book is dedicated to the memory of Professor Józef Joachim Telega (1943–2005) who carried the burden of his illness with exemplary bravery. Throughout his life, he devoted his outstanding intellectual capacity with enormous energy and persistence to the mathematical treatment of problems of mechanics, in particular of biomechanics.

This text is meant to serve as an introduction and overview for students with an interest in biomechanics. Its purpose is to demonstrate the wide range of mathematical principles and procedures which are necessary to cover the enormously large field of biomechanics which extends from molecular to macroscopic dimensions. Mathematical rigor and completeness of theories including the derivation of formulas are thereby not in the foreground, rather, it is attempted to present the material in a concise, easy to follow fashion and provide the student with a working knowledge. It is however assumed that the reader is familiar with the basic principles of analysis and linear algebra.

Biomechanics, as an interdisciplinary field, has numerous connections and overlapping areas with mathematics and physics on the one hand, and with biology, physiology, pathophysiology as well as clinical medicine on the other. Even a partial treatment of the subject is hardly possible for one single author. Accordingly, this text contains selected material which covers basic theoretical principles of general validity as well as specific applications serving as illustrative examples without going into details.

Peter F. Niederer
Zurich, November 2005

niederer@biomed.ee.ethz.ch

Chapter 1

Introduction

Rigid Bodies $\Leftrightarrow$ Continua

The science of biomechanics is concerned with the quantitative analysis of the mechanical behavior of biological systems. The range of the systems of interest thereby extends from the molecular to the macroscopic level. In order to arrive at useful results and practical applications, the classical engineering methods are being applied, i.e. measurements performed on the real system or on a laboratory model, as well as mathematical analysis and modeling of a usually simplified system which is representative and exhibits all features of interest.

Real bodies, solid or fluid (the latter liquid or gaseous), undergo deformations when forces act on them. In case that the vectorial sum of all the external forces is different from zero, the center of mass of the body is furthermore accelerated, and, if the moment is not zero, there will be rotational accelerations.

The first step in any mechanical analysis consists of outlining the system under consideration. This may then be composed of numerous solid of fluid bodies which interact with or are independent from one another. Under all circumstances, however, the system as a whole has a common center of mass which obeys Newton's second law of motion ("principle of solidification").

Yet, the various components of a system may exhibit marked differences with respect to deformations and accelerations. Particularly important differences exist between solids and fluids which have to be taken into account in their mathematical description. Since biological bodies always consist of

solid and fluid materials, the entire range of classical mechanics is needed for their modeling (we disregard aspects of quantum mechanics and relativity in this book, since masses, dimensions and velocities of interest here are outside the range where such theories are of importance).

Under a given loading pattern, the size of the deformations of biological solids depends on the deformability of the material(s) the body consists of while accelerations are determined by masses and moments of inertia. To some extent, deformations and accelerations can be treated independently from one another. Fluids, in contrast to solid bodies, have no fixed reference configuration in that fluid particles can rearrange themselves to a large extent freely. A separation of deformation and displacement is physically not meaningful.

In biomechanics, a distinction is often made between "soft" and "hard" tissues. Soft tissues include, e.g., muscle, skin, liver, brain, connective tissue, etc., whereas hard tissue is generally calcified (bone). Within the framework of a linearized Hookean approximation, the Young's modulus of soft and hard tissues differs by orders of magnitude in that typical soft tissues have a modulus of elasticity between some ten kPa and several hundred kPa, while in the case of hard tissue it is way up in the hundred MPa range. Accordingly, the deformations that the different tissues experience in daily life differ greatly. This is reflected consequently in the wide range of mathematical treatment strategies which are applied to analyze the phenomena of interest in biomechanics.

Under physiological loading conditions, the skeleton deforms little, otherwise, injury may occur. For many purposes, therefore, in particular for motion analysis, the human body may be approximated as a system of rigid bodies. A rigid body is an approximation which is useful whenever deformations are sufficiently small in comparison with the displacements which the body under consideration executes and whenever they are moreover not of interest for the problem at hand. This approximation has an important mathematical consequence. A rigid body moving freely in space has six degrees of freedom which implies that the position and orientation in space can uniquely be determined by 6 generalized coordinates. Likewise, any system consisting of a finite number of rigid bodies has a finite number of degrees of freedom. Their exact number depends on the connectivity of the system as well as on eventual external constraints that have to be observed. The equations of motion that describe the system are ordinary differential equations,

mostly nonlinear, with singularities if collisions are modeled. The number of independent equations thereby corresponds to the number of degrees of freedom.

As molecular and cellular aspects gain increasing importance in biomechanics, methods of molecular dynamics and modeling are more and more applied for the analysis of physiological problems. The procedures used in these approaches are largely based on rigid body dynamics, in fact, the mechanics of mass points are often applied. Thanks to the enormous increase in computational power, e.g., the interaction and functional behavior of large biomolecules can be studied. A great number of simultaneous equations has often to be treated thereby.

The concept of a continuum implies in turn that any part of the body, regardless how small it may be, still has an infinite number of degrees of freedom (the atomistic nature of any substance is disregarded). Whenever deformations of a solid body are of interest or in the case of fluid flow, an analysis based on continuum mechanics is required since any kind of distortion, solid or fluid is continuous in nature. Local noncontinuities (disruptions) or non differentiable regions in deformation or flow fields (e.g., shock waves) may nevertheless occur. The equations to be solved are partial differential equations.

Physiological processes in the human body take generally place within a relatively small temperature interval around 37.5°C. For many purposes, therefore, isothermal conditions can be assumed and thermodynamics need not be taken into account. Yet, diffusive processes including osmosis play an important role in biology (also in biomechanics) such that statistical mechanics or certain aspects of thermodynamics have nevertheless to be considered if such processes are to be understood. Also energy balances associated with physiologic processes from a molecular to a macroscopic level are subjected to the laws of thermodynamics.

Systems investigated in biomechanics (organs, cells, etc.) are characterized in general by an irregular geometry and complex nonlinear mechanical properties. An analysis based on analytic solutions of differential equations is mostly not possible; computational procedures are therefore of primary importance. Nevertheless, simplified models which allow for closed form solutions are often helpful in order to obtain insight into the general properties of a system; in particular, a sensitivity analysis with respect to the influence of system parameters can readily be made. In contrast, a numerical solution

always represents a particular case and does not necessarily reflect a basic behavior. In order to derive general properties, numerous calculations and a time consuming procedure are often necessary.

Chapter 2

Rigid Body Dynamics

2.1. Basic Kinematics

Rigid body approximations have various applications in biomechanics, in particular for human or animal motion analysis, for molecular modeling or for a simplified preliminary investigation of an otherwise complicated process in general. In most cases, systems of rigid bodies are considered which are connected in joints (e.g., a model for the human body) or have interactions through external forces (e.g., molecules).

An unrestrained rigid body has 6 degrees of freedom in space which are parameterized by 6 quantities (generalized position coordinates). The particular parameterization of use is determined according to the problem to be solved; e.g., 3 linear Cartesian coordinates x_1, x_2, x_3 denoting the location of the center of mass $\mathbf{r} = x_1\mathbf{e}_1 + x_2\mathbf{e}_2 + x_3\mathbf{e}_3$ in a reference system with orthogonal unit vectors $(\mathbf{e}_1, \mathbf{e}_2, \mathbf{e}_3)$, and 3 angles (specified later) [1] are chosen. In the following, we will use for brevity the matrix notation

$$\mathbf{r} = \begin{bmatrix} x_1 \\ x_2 \\ x_3 \end{bmatrix}$$

to denote a vectorial quantity (although, mathematically correct, vectors and

[1] Throughout this book, we restrict ourselves to rectangular coordinate systems, such as Cartesian, cylindrical or spherical systems. Scalar quantities are denoted with italics, vectors with lowercase bold letters and tensors of higher rank with bold uppercase letters.

their components in a coordinate system have to be clearly distinguished and

$$\mathbf{r} = \begin{bmatrix} x_1 \\ x_2 \\ x_3 \end{bmatrix} [\mathbf{e}]$$

would have to be written using the base vectors, abbreviated here symbolically by [**e**]).

As such, the body is characterized by its position and orientation in space with respect to an inertial reference system. The inertial properties, to be used later, are furthermore given by the mass m and the moment of inertia tensor $\mathbf{I}$. The shape or outer contour of the body has to be considered when collision problems are to be solved, whereas the interior structure is generally not of importance. If the number of degrees of freedom is reduced due to constraints, the number of generalized coordinates is reduced accordingly.

Besides an inertial reference, it is often useful to introduce other reference systems, e.g., a body-fixed system, because, as the body executes some motion in space, the components of the moment of inertia tensor are constant in time with respect to such a system. Its location and spatial orientation change with time however, and they have to be related to the inertial reference system, since the equations of motion have to be formulated in inertial coordinates (each reference system is associated with a coordinate system where a complete set of generalized coordinates is defined; in the following, Cartesian coordinates are assumed). Accordingly, we have to establish transformations between coordinate systems which may depend on time.

Two coordinate systems can always be made to coincide by a translation and a rigid rotation in that, first, the two origins are brought together by a translation; second, a sequence of rotations is made such that the axes (or direction of base vectors) coincide. While the translation is given by a spatial vector, the rotation is described by a matrix since the relation between the coordinates can be expressed as a linear mapping. In order to investigate the properties of this matrix, we make use of the fact that a given vector,

$$\mathbf{c} = \begin{bmatrix} c_1 \\ c_2 \\ c_3 \end{bmatrix},$$

has the same length $|\mathbf{c}| = \sqrt{(\mathbf{c} \cdot \mathbf{c})}$ when it is decomposed in another coordinate system (inertial or arbitrarily moving in space). The scalar product,

$(\mathbf{c} \cdot \mathbf{c})$, is thereby defined as the matrix product

$$\begin{bmatrix} c_1 \\ c_2 \\ c_3 \end{bmatrix}^{\mathsf{T}} \cdot \begin{bmatrix} c_1 \\ c_2 \\ c_3 \end{bmatrix} = [c_1, c_2, c_3] \cdot \begin{bmatrix} c_1 \\ c_2 \\ c_3 \end{bmatrix}$$

Scalar products are indicated by a dot and the superscript $^{\mathsf{T}}$ denotes a transposition [2].

The components of the vector $\mathbf{c}$, written in two different coordinate systems (Fig. 2.1),

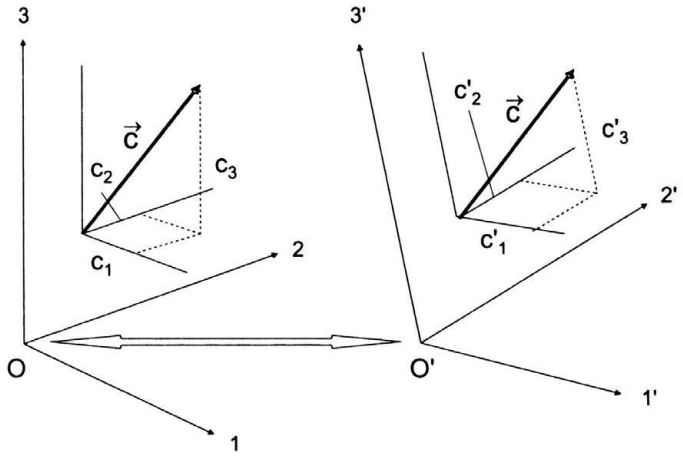

FIGURE 2.1. Vector $\mathbf{c}$ decomposed in two different coordinate systems. For clarity, the two coincident origins, O and O', respectively, are displaced.

$$\begin{bmatrix} c_1 \\ c_2 \\ c_3 \end{bmatrix} \quad \text{and} \quad \begin{bmatrix} c'_1 \\ c'_2 \\ c'_3 \end{bmatrix},$$

respectively, are related by a linear mapping

$$\begin{bmatrix} c_1 \\ c_2 \\ c_3 \end{bmatrix} = \mathbf{D} \cdot \begin{bmatrix} c'_1 \\ c'_2 \\ c'_3 \end{bmatrix} = \begin{bmatrix} d_{11} & d_{12} & d_{13} \\ d_{21} & d_{22} & d_{23} \\ d_{31} & d_{32} & d_{33} \end{bmatrix} \cdot \begin{bmatrix} c'_1 \\ c'_2 \\ c'_3 \end{bmatrix}. \tag{2.1}$$

[2] Although covariant and contravariant components are the same for rectangular coordinate systems, it is useful to distinguish between column and row vectors such that the rules of matrix multiplication for scalar and vector products can be applied.

Again, as for vectors, the abbreviated matrix notation

$$\mathbf{D} = \begin{bmatrix} d_{11} & d_{12} & d_{13} \\ d_{21} & d_{22} & d_{23} \\ d_{31} & d_{32} & d_{33} \end{bmatrix}$$

is used to indicate tensors instead of the correct symbolic notation

$$\mathbf{D} = \left[\mathbf{e}^{\mathsf{T}}\right] \begin{bmatrix} d_{11} & d_{12} & d_{13} \\ d_{21} & d_{22} & d_{23} \\ d_{31} & d_{32} & d_{33} \end{bmatrix} [\mathbf{e}] .$$

A first property of $\mathbf{D}$ is obtained from the condition of invariant length, i.e.,

$$\mathbf{c} \cdot \mathbf{c} = (\mathbf{D}\mathbf{c}') \cdot (\mathbf{D}\mathbf{c}') \tag{2.2}$$

from which follows

$$\mathbf{D}^{\mathsf{T}} \cdot \mathbf{D} = \mathbf{1} \quad \text{as well as} \quad \det \mathbf{D} = 1. \tag{2.3}$$

Accordingly, the matrix $\mathbf{D}$ is orthogonal and its determinant is equal to 1.

If $\mathbf{D}$ relates e.g. a body fixed to an inertial reference system, it will in general depend on time. It can therefore be differentiated with respect to time and one finds from Eq. (2.3a)

$$\frac{d}{dt}\left(\mathbf{D}^{\mathsf{T}} \cdot \mathbf{D}\right) = \mathbf{D}^{\mathsf{T}} \cdot \dot{\mathbf{D}} + \dot{\mathbf{D}}^{\mathsf{T}} \cdot \mathbf{D} = \mathbf{D}^{\mathsf{T}} \cdot \dot{\mathbf{D}} + \left(\mathbf{D}^{\mathsf{T}} \cdot \dot{\mathbf{D}}\right)^{\mathsf{T}} = 0. \tag{2.4}$$

Upon defining $\mathbf{D}^{\mathsf{T}} \cdot \dot{\mathbf{D}} = \boldsymbol{\Omega}$, (2.4) yields $\boldsymbol{\Omega} = -\boldsymbol{\Omega}^{\mathsf{T}}$ which implies that $\boldsymbol{\Omega}$ can be written in the form

$$\boldsymbol{\Omega} = \begin{bmatrix} 0 & -\omega_3 & \omega_2 \\ \omega_3 & 0 & -\omega_1 \\ -\omega_2 & \omega_1 & 0 \end{bmatrix}. \tag{2.5}$$

(The choice of the signs and of the indices will be justified later.) From the definition of $\boldsymbol{\Omega}$ one finds furthermore the important relation

$$\dot{\mathbf{D}} = \mathbf{D} \cdot \boldsymbol{\Omega}. \tag{2.6}$$

We now look at a fixed point P, on the moving body at time t and $t + \Delta t$, respectively. The body fixed vector, PP_0 is denoted by $\mathbf{b}$. From Fig. 2.2 it is seen that the relation holds

$$\mathbf{r}(t) + \mathbf{b}(t) + \Delta\mathbf{r}\,(t + \Delta t) = \mathbf{r}\,(t + \Delta t) + \mathbf{b}\,(t + \Delta t)$$

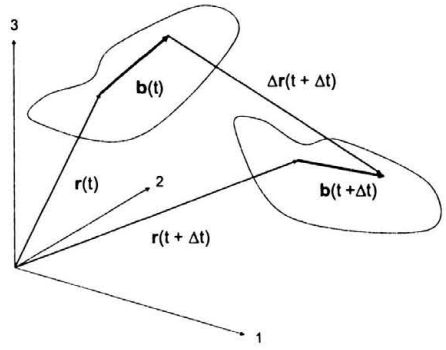

FIGURE 2.2. Motion of a rigid body in space with a body-fixed vector $\mathbf{b}$

or

$$\mathbf{r}(t) + \mathbf{b}(t) + \frac{d(\Delta\mathbf{r}(t))}{dt}\Delta t = \mathbf{r}(t) + \frac{d(\mathbf{r}(t))}{dt}\Delta t + \mathbf{b}(t) + \frac{d(\mathbf{b}(t))}{dt}\Delta t$$

for small Δt. Accordingly, with $\Delta t \to 0$, we obtain

$$\frac{d(\Delta\mathbf{r})}{dt} = \mathbf{v}(P) = \frac{d\mathbf{r}}{dt} + \frac{d\mathbf{b}}{dt} = \mathbf{v}(P_0) + \frac{d\mathbf{b}}{dt}.$$

But, using $\dot{\mathbf{b}} = \dot{\mathbf{D}} \cdot \mathbf{b} = \mathbf{D} \cdot \boldsymbol{\Omega} \cdot \mathbf{b}$ and observing that for $\Delta t \to 0$, $\mathbf{D} \to \mathbf{1}$, we arrive at

$$\mathbf{v}(P) = \mathbf{v}(P_0) + \boldsymbol{\Omega} \cdot \mathbf{b} = \mathbf{v}(P_0) + \boldsymbol{\omega} \times \mathbf{b} \tag{2.7}$$

with the angular velocity vector

$$\boldsymbol{\omega} = \begin{bmatrix} \omega_1 \\ \omega_2 \\ \omega_3 \end{bmatrix}.$$

The definition of the components of $\boldsymbol{\Omega}$ has previously made such that the angular velocity vector appears in the well known form given above.

We turn our attention now to the parameterization of the orthogonal matrix

$$\begin{bmatrix} d_{11} & d_{12} & d_{13} \\ d_{21} & d_{22} & d_{23} \\ d_{31} & d_{32} & d_{33} \end{bmatrix}.$$

Since the group of spatial rotations is noncommutative, care has to be taken in the choice of an appropriate form, and in fact various formulations have been used in the past depending on the problem at hand.

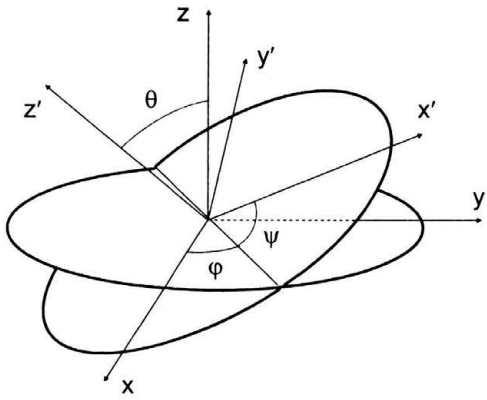

FIGURE 2.3. Definition of Euler angles

The oldest form, useful to describe gyroscopes, was introduced by Euler: the three Euler angles (Fig. 2.3) (φ, θ, ψ) characterize a rotation around a body axis (self rotation, $\dot{\psi}$, if the body has the largest principal axis at rest in z-direction), a precession $(\dot{\varphi})$ and a nutation $(\dot{\theta})$. It is thereby implicitly assumed that the rotations are related to a fixed point in space. Upon applying the transformations

$$\mathbf{D}_1 = \begin{bmatrix} \cos\varphi & \sin\varphi & 0 \\ -\sin\varphi & \cos\varphi & 0 \\ 0 & 0 & 1 \end{bmatrix}; \quad \mathbf{D}_2 = \ldots; \quad \mathbf{D}_3 = \ldots$$

(the first describes the rotation around φ, the associated matrices for the rotation around the other two angles can be found by interchanging the rows and columns accordingly and replacing the angles) in the indicated sequence, one finds by matrix multiplication

$$\mathbf{D} = \begin{bmatrix} \cos\psi\cos\varphi - \cos\theta\sin\varphi\sin\psi & \cos\psi\sin\varphi + \cos\theta\cos\varphi\sin\psi & \sin\psi\sin\theta \\ -\sin\psi\cos\varphi - \cos\theta\sin\varphi\cos\psi & -\sin\psi\sin\varphi + \cos\theta\cos\varphi\cos\psi & \cos\psi\sin\theta \\ \sin\theta\sin\varphi & -\sin\theta\cos\varphi & \cos\theta \end{bmatrix}$$

Since the angles φ and ψ are not readily defined for $\theta = 0$, the Euler angles are not particularly useful for the description of spatial rigid body motions, in particular, if numerical applications are made.

Similarly, the expressions *yaw, pitch,* and *roll* which are adapted from nautical language denote rotations around the three orthogonal axes of a fixed

reference system. **D** can again be found by multiplication of three successive rotations.

A more general formulation (from the point of view of applications) can be found if the two coordinate systems under consideration are related by a rotation with an angle ϑ around a fixed axis which is given by a unit vector $\boldsymbol{\mu}$, ($|\boldsymbol{\mu}| = 1$) (this is called a simple rotation). By executing, if necessary, a suitable translation, this can always be achieved. From Fig. 2.4 we find that

$$\mathbf{D} = \mathbf{1}\cos\vartheta - \mathbf{1}\times\boldsymbol{\mu}\sin\vartheta + \boldsymbol{\mu}\otimes\boldsymbol{\mu}\,(1-\cos\vartheta)\,. \tag{2.8}$$

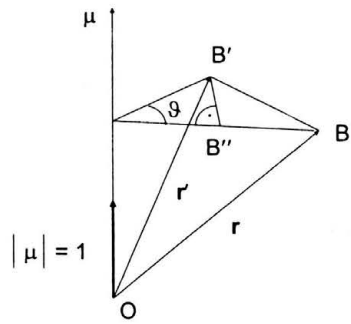

FIGURE 2.4. Simple rotation: $\mathbf{r}' = \vec{OC} + \vec{CB''} + \vec{B''B'}$, $\vec{OC} = \boldsymbol{\mu}(\boldsymbol{\mu}\cdot\mathbf{r}) = \boldsymbol{\mu}\boldsymbol{\mu}^{\mathsf{T}}\mathbf{r}$, $\vec{CB''} = \cos\vartheta(\mathbf{1} - \boldsymbol{\mu}\boldsymbol{\mu}^{\mathsf{T}})\mathbf{r}$, $\vec{B''B'} = -\sin\vartheta\boldsymbol{\mu}\times\mathbf{r}$

The symbol $\otimes$ denotes a dyadic product and

$$\mathbf{1}\times\boldsymbol{\mu} = \begin{bmatrix} 0 & -\mu_3 & \mu_2 \\ \mu_3 & 0 & -\mu_1 \\ -\mu_2 & \mu_1 & 0 \end{bmatrix}.$$

The four quantities $\boldsymbol{\mu}$, ϑ are not independent because of $|\boldsymbol{\mu}| = 1$. With the aid of the expression

$$\varepsilon_{ijk} = \frac{1}{2}(i-j)(j-k)(k-i)\,, \quad i,j,k = 1,2,3$$

as well as the Kronecker symbol δ_{ij} the components of the matrix associated with **D** are obtained as

$$d_{ij} = \delta_{ij}\cos\vartheta - \sum_k \varepsilon_{ijk}\mu_k\sin\vartheta + \mu_i\mu_j\,(1-\cos\vartheta)\,. \tag{2.9}$$

A further useful relation is based on direction cosines. Two coordinate systems with base vectors $\mathbf{e}_i$ and $\mathbf{e}'_i$, respectively are related by the cosines $c_{ij} = \left(\mathbf{e}_i, \mathbf{e}'_j\right)$ in the form

$$\mathbf{D} = \begin{bmatrix} c_{11} & c_{12} & c_{13} \\ c_{21} & c_{22} & c_{23} \\ c_{31} & c_{32} & c_{33} \end{bmatrix}. \tag{2.10}$$

This relation is found by decomposition of the base vectors of one system with respect to the other.

For completeness, two further parametrizations are mentioned. A representation using quaternions is obtained if the definitions

$$\varepsilon = \boldsymbol{\mu} \sin\left(\frac{\vartheta}{2}\right) \quad \text{and} \quad \varepsilon_4 = \cos\left(\frac{\vartheta}{2}\right)$$

are introduced. Since $\sum_{i=1}^{4} \varepsilon_i^2 = 1$, the 4 quantities have the properties of quaternions. If this representation is used, the quaternion property has to be restored after each integration step. This disadvantage is however offset by the fact that this involves a fitting procedure which adds to the stability of the integration.

Directly related with the quaternions are the three Rodrigues parameters

$$\rho_i = \frac{\varepsilon_i}{\varepsilon_4}, \quad i = 1, 2, 3.$$

Since these parameters can become infinite, they are usually not used in numerical procedures.

Two of the representations outlined above ($\boldsymbol{\mu}$, ϑ and direction cosines) are well suited for numerical applications which involve the integration of linear and angular accelerations. Accordingly, the time derivative of $\mathbf{D}$ or an expression for $\boldsymbol{\omega}$, respectively, are needed in terms of the parameters.

While in the case of the direction cosine parameterization, Eq. (2.6) can be used directly, Eqs. (2.6), (2.8) and (2.9) yield, after some calculation,

$$\begin{aligned} \dot{\vartheta} &= (\boldsymbol{\omega} \cdot \boldsymbol{\mu}), \\ \dot{\boldsymbol{\mu}} &= \frac{1}{2}\boldsymbol{\omega} \times \boldsymbol{\mu} - \frac{\sin\vartheta}{2\,(1 - \cos\vartheta)} (\boldsymbol{\omega} \times \boldsymbol{\mu}) \times \boldsymbol{\mu}. \end{aligned} \tag{2.11}$$

Once $\boldsymbol{\omega}$ is determined from the equations of motion (see below), the direction matrices can be updated along with the position vectors.

2.2. Measurement Methods

The measurement of human body motions is mostly based on optical methods (position measurements) or on the application of acceleration sensors (Fig. 2.5). While velocities and accelerations from position measurements are obtained by differentiation, accelerations have to be integrated in order to determine velocities and positions. In case of differentiation, noise amplification is a well known problem, and appropriate filters have to be applied in order to ascertain recording of the useful signal contents. Linear accelerometers, in turn, which measure accelerations in one direction can be made small and light-weight; the measurement of angular or rotational accelerations is in contrast more critical although angular accelerometers for various measurement ranges and purposes exist.

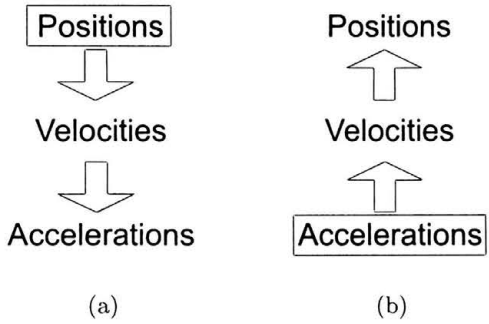

FIGURE 2.5. Measurement on the basis of positions (a) or accelerometers (b)

It is sometimes attempted to obtain angular accelerations with the aid of a combination of linear accelerometers. Since these elements are usually fixed on the human limbs and therefore change their orientation, i.e., their measurement direction in space when the body moves, the term "strap-down" measurement is used. Under such conditions, linear and angular accelerations with respect to inertial reference cannot be obtained in a straightforward manner. A problem exists in particular because accelerometers always sense gravity and a signal is recorded already when a linear accelerometer is rotated with respect to the direction of gravity.

We consider the output of a linear accelerometer which moves in space. According to (2.7), after differentiation with respect to time, we obtain for the acceleration $\mathbf{a}$, measured at a fixed point P on the body

$$\mathbf{a}(P) = \mathbf{a}(P_0) + \dot{\boldsymbol{\omega}} \times \mathbf{b} + \boldsymbol{\omega} \times \boldsymbol{\omega} \times \mathbf{b} \tag{2.12}$$

in relation to a reference point P_0 on the same limb (the distance $PP_0 = |\mathbf{b}|$ has to be constant in time). Theoretically, 6 independent measurements $\mathbf{a}_i(P_i)$ suffice to determine $\mathbf{a}(P_0)$ and $\boldsymbol{\omega}$ if the distances P_iP_0 are known (the points P_i have thereby to be chosen appropriately, in particular, collinearity has to be avoided). Due to the fact however, that $\boldsymbol{\omega}$ appears in quadratic form in Eq. (2.12), this procedure is associated with intolerable errors.

With a minimum of 9 linear accelerometers, which are arranged according to the scheme shown in Fig. 2.6, the quadratic terms can be eliminated (definition of symbols according to Fig. 2.6). In direction x the measurements read

$$a_i = a_{x0} + \dot{\omega}_y z_i - \dot{\omega}_z y_i + \omega_x \left(\omega_y y_i + \omega_z z_i\right), \quad i = 1, 2, 3, \quad x_i = 0,$$

y_i, z_i denote the location of the accelerometers.

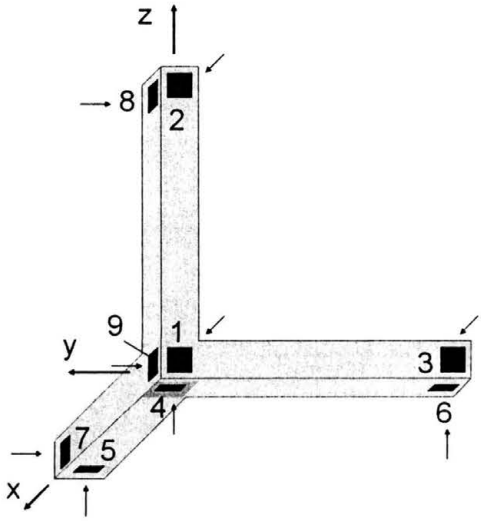

FIGURE 2.6. Configuration of linear accelerometers when 9 accelerometers are used for the recording of spatial motions. The small arrows indicate the positive direction.

The other two directions (y, z) yield similar formulas (the $\pm$orientation of the accelerometer has thereby to be observed). Upon substituting for the quadratic terms, one arrives at

$$
\begin{aligned}
2\dot{\omega}_x &= \frac{a_8 - a_9}{z_8 - z_9} + \frac{a_6 - a_4}{y_6 - y_4}, \\
2\dot{\omega}_y &= \frac{a_2 - a_1}{z_2 - z_1} - \frac{a_5 - a_4}{x_5 - x_4} - \frac{(a_3 - a_1)(y_2 - y_1)}{(y_3 - y_1)(z_2 - z_1)}, \\
2\dot{\omega}_z &= \frac{a_7 - a_9}{x_7 - x_9} + \frac{a_3 - a_1}{y_3 - y_1}.
\end{aligned} \tag{2.13}
$$

These equations can readily be integrated, however, a drift problem occurs. This is not the case if position measurements are made. A drawback nevertheless exists because by the differentiation and necessary filtering process bandwidth is lost, accordingly, high speed recording requiring intensive light is necessary. In contrast, the bandwidth of accelerometers is sufficient for all practical purposes.

2.3. Dynamics

Most dynamic phenomena of interest in biomechanics are such that their complexity does not allow for an analytic treatment, rather, numerical procedures have to be applied. Accordingly, the following considerations are restricted in view of computer modeling. For further analysis, the reader is referred to the books [1, 2].

The analysis of rigid body motion is based on linear and angular momentum balance. For each rigid body of a system (N is a number of bodies or segments), the following two equations hold: the momentum equation:

$$
m_n \ddot{\mathbf{r}}_n = \sum_k \hat{\mathbf{f}}_{nk} + \sum_j \mathbf{f}_{nj}, \quad n = 1, \ldots, N \tag{2.14}
$$

where:

m_n is the mass of rigid segment n,

$\mathbf{r}_n$ is the center of mass of segment n,

$\hat{\mathbf{f}}_{nk}$ is the force k, acting on segment n,

$\mathbf{f}_{nj}$ is the force of the joint j, acting on segment n.

In body-fixed reference for each segment n, the angular momentum balance is

$$\mathbf{I}_n \cdot \dot{\boldsymbol{\omega}}_n = -\boldsymbol{\omega}_n \times (\mathbf{I}_n \boldsymbol{\omega}_n) + \mathbf{D}_n \cdot \left(\sum_k \mathbf{D}_n^{-1} \cdot \boldsymbol{\rho}_{nk} \times \hat{\mathbf{f}}_{nk} + \sum_j \mathbf{D}_n^{-1} \cdot \boldsymbol{\kappa}_{nj} \times \mathbf{f}_{nj} + \sum_l \mathbf{D}_n^{-1} \cdot \mathbf{t}_{nl} + \sum_m \boldsymbol{\tau}_{nm} \right) \quad (2.15)$$

where:

$\mathbf{I}_n$ is the inertia tensor of segment n in body-fixed reference,

$\boldsymbol{\omega}_n$ is the angular velocity of segment n,

$\mathbf{D}_n^{-1}$ is the transformation from body-fixed into inertial system,

$\boldsymbol{\rho}_{nk}$ is the point of application of the external force $\hat{\mathbf{f}}_{nk}$,

$\boldsymbol{\kappa}_{nj}$ is the point of application of joint force $\mathbf{f}_{nj}$,

$\mathbf{t}_{nl}$ is the torque l, acting on segment n, due to joint constraints,

$\boldsymbol{\tau}_{nm}$ external torque m, acting on segment n.

The term on the left side of Eq. (2.15) and the first term on the right side originate from

$$\frac{d}{dt} \left(\mathbf{D}_n^{-1} \mathbf{I}_n \boldsymbol{\omega}_n \right)$$

where the relation (2.6) has been used. This is a useful formulation since the inertia tensor $\mathbf{I}$ is constant in a body-fixed system; the equation is written in inertial reference, however. The entire equation is finally multiplied with $\mathbf{D}_n$ in order to transform it onto body-fixed reference.

In addition to these basic equations, there are usually a number of constraints due to joints (ball and socket, hinge, etc.) and external conditions (e.g., sliding along a plane). All of these constraints are assumed to appear in the form

$$f\left(\mathbf{D}_n, \mathbf{r}_n, \dot{\mathbf{r}}_n, \text{angles}, \boldsymbol{\omega}_n, \text{external parameters}\right) = 0 \quad (2.16)$$

with first order time derivatives at most [3]. These equations are added to the basic equations of motion and the entire set can directly be utilized for numerical integration. The constraints reduce the degree of freedom of the system and the first step during the integration procedure of Eqs. (2.14–2.16) consists therefore of eliminating "superfluous" variables. Although this

[3] In case of viscoelastic damping, a hereditary integral may be involved.

complicates the method, an important advantage consists of the flexibility which is maintained in that changes of the model, of the connectivity of a rigid body system, of joint properties or of external constraint can readily be implemented. Likewise, quantities in inertial or body-fixed reference are easily calculated (Example I).

An approach based on the Lagrangian formulation leads to M equations (number of degrees of freedom of the entire system, each degree of freedom is thereby parameterized by a generalized coordinate q_k) for the system consisting of N bodies

$$\frac{d}{dt}\left(\frac{\partial T}{\partial \dot{q}_k}\right) - \frac{\partial T}{\partial q_k} = \frac{\partial V}{\partial q_k} + Q_k, \quad k = 1, \ldots, M. \tag{2.17}$$

The kinetic energy is

$$2T = \sum_{n=1}^{N} m_n \left(\mathbf{v}_n \cdot \mathbf{v}_n\right) + \sum \left(\boldsymbol{\omega}_n \cdot \left(\mathbf{I}_n \cdot \boldsymbol{\omega}_n\right)\right)$$

and V denotes a potential. The generalized forces Q_k include forces which cannot be described by a potential and have to be derived with the aid of the principle of virtual work *(note: also internal forces may contribute, e.g., friction)*.

This approach leads to a minimal set of equations because all the constraints are included in the formulation. The disadvantage derives from the lack of flexibility such that this method is usually not used in general purpose programs.

Other procedures have been proposed and can be found in the literature; the two methods outlined here are however the most important (and are moreover the basis for other formulations). For the numerical integration an integrator which is adapted for stiff equations is needed. After each integration step, the orthogonality of the transformation matrices has usually to be restored by a fitting procedure. A simple (but not exhaustive) control can be made by following the common center of mass of the system under consideration which has to execute a linear, constant motion if external forces are absent. Likewise, an energy balance can be performed.

An important aspect is related to the sensitivity of the calculated results with respect to the initial conditions and system parameters. Small changes in the initial conditions or in the values of the system parameters may sometimes lead to large deviations and variability of the resulting motions, in particular

in case of collisions. Often, numerous parametric variations are necessary in order to validate the significance and usefulness of a simulation.

Collisions may cause difficulties in that within the framework of rigid bodies, collisions lead to singularities (infinite forces acting over an infinitely short period of time). There are in essence two ways to deal with this problem. First, the bodies are "softened" such that there are no infinite forces. To this end, a force-penetration model is developed for which the outer contours of the segments are needed. Mutual penetration can readily be calculated from the centers of mass and orientation matrices. Second, each collision configuration is determined exactly (machine precision) by interpolation and the collision is bridged with the aid of conservation laws.

2.4. Molecular Modeling

Atoms interact with one another primarily through their atomic shells consisting of electrons. Covalent bindings, e.g., derive from a direct interaction of electrons. Likewise, ionic bonds are based on electron exchange. Along with the nuclei, dipole effects are furthermore of importance, in addition, noncovalent bonds, hydrogen bridges, van der Waals forces, hydrophilic-hydrophobic interactions (of particular importance for biomolecules), in case of metallic materials still other effects, excited electronic states, interactions with electromagnetic fields, etc., have to be taken into account.

The electron mass and dimensions under consideration are such that the principles of quantum mechanics, in particular the Schrödinger equation has to be applied for the analysis of atomic systems. This equation incorporates the probability function $\Psi(\mathbf{r}, t)$, i.e., the wave function describing the probability that a particle is at a certain location $\mathbf{r}$ at time t; the volume integral satisfies $\int |\Psi|^2 dV = 1$ as is required for probabilities.

$$\mathrm{i}\hbar \frac{\partial \Psi}{\partial t} = -\frac{\hbar}{2m} \nabla^2 \Psi(\mathbf{r}, t) + V(\mathbf{r}, t)\, \Psi(\mathbf{r}, t)\,. \tag{2.18}$$

Here m denotes the mass of the particle whose probability distribution is calculated, ∇^2 the Laplace operator, $\hbar$ is Planck's constant divided by 2π, $V(\mathbf{r}, t)$ is a potential, and $\mathrm{i} = \sqrt{-1}$.

A solution of this equation for a system involving a large number of atoms is not possible with present computational techniques; yet, it is not necessary for many particularly interesting (from the standpoint of biomechanics)

applications. Such applications involve, e.g., the interaction and functional properties of large protein molecules including their behavior under the influence of forces.

A usual procedure of treating the Schrödinger equation consists of introducing a separation ansatz

$$\Psi(\mathbf{r}, t) = \psi(\mathbf{r}) \cdot \mathrm{e}^{-\frac{\mathrm{i}Et}{\hbar}}$$

into Eq. (2.18) which leads to the time-independent Schrödinger equation

$$H\psi = E\psi \tag{2.19}$$

with the Hamiltonian (energy) operator $H = -\frac{\hbar}{m}\nabla^2 + V$ and the energy E.

Next, the Born-Oppenheimer approximation is applied. Since the mass of an electron is more than three orders of magnitude smaller than the mass of a nuclear particle (proton or neutron), the motion of the nucleus can be assumed to be independent of the motion of the electrons. A further factorization is therefore possible. This approximation allows to model the electrons in a summary fashion as a static cloud and replace their influence by a potential function which mimics the forces which they cause upon interaction with neighboring atoms (see below).

According to Ehrenfest's theorems, furthermore, the expectation values of the Schrödinger wave function Ψ obey the laws of classical mechanics. In case that the de Broglie wavelength $\lambda = \sqrt{2\pi\hbar^2/(mkT)}$ (k denotes Boltzmann's constant, T the absolute temperature) is small in comparison with the typical dimension of the problem under investigation (e.g., atom-atom distances), molecular dynamics can therefore adequately be described by classical mechanics. Already the mass of a helium atom ($\approx 10^{-26}$ kg) is sufficiently large that this approximation is justified.

Since atomic nuclei are small in comparison with molecular dimensions, "simple" point mass mechanics can be applied for each element i (mass m_i, location $\mathbf{r}_i(t)$)

$$m_i \frac{d^2\mathbf{r}_i}{dt^2} = \sum_k \mathbf{f}_{ik}. \tag{2.20}$$

While this is rather straightforward, the formulation of the interacting forces ($\sum \mathbf{f}_{ik}$, k extends over all interactions), i.e., the derivation of potential functions representing the electrons within the framework of the Born-Oppenheimer approximation is not, since this has to be derived from quantum

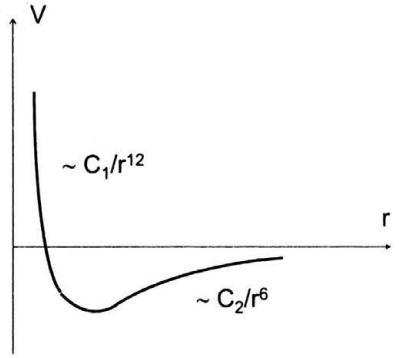

FIGURE 2.7. Lennard-Jones potential (schematically)

mechanics or empirical knowledge. A large body of literature can be found on this difficult and crucial subject. A typical potential, which is often used, is the Lennard-Jones potential which may serve as an example

$$V = C_1 \left(\left[\frac{C_2}{r_{ij}} \right]^{12} - \left(\frac{C_2}{r_{ij}} \right)^6 \right). \tag{2.21}$$

This potential (Fig. 2.7) describes the strong repulsion ($\propto r^{-12}$) that atoms are exposed to when their electron clouds are overlapping as well as the van der Waals attraction at larger distances ($\propto r^{-6}$). C_1 and C_2 are constants which have to be fitted according to the specific interaction to be modeled.

A further problem arises from long range interactions such as electrostatic forces which exhibit a $1/r$ dependence. Accordingly, in a large system, all particles can in principle interact and many-body interactions can occur. In case of thousands of particles, this leads to an untreatable complexity such that further approximations are necessary.

Two circumstances render molecular dynamics simulations expensive (computer hardware) and time consuming. First, the number of particles along with their interactions may be very large. Second, typical integration steps are of the order of 10^{-15} to 10^{-14} sec. This small step size is given by the internal dynamics of the molecules, e.g., vibrations. An enormous number of integration steps have therefore to be made in order to reach useful time spans. Verlet or Gear-type integrators which are adapted for stiff equations are mostly used.

Thanks to the rapid increase of computational power, large molecules, in particular biomolecules including the environment consisting of a large number of water molecules are amenable to a simulation (Example II).

References

1. J. WITTENBURG, *Dynamics of Systems of Rigid Bodies*, Teubner, Stuttgart 1977

2. TH. KANE, *Spacecraft Dynamics*, Mcgraw-Hill 1981

Chapter 3

Continuum Mechanics

3.1. Deformations: Strain

We consider an arbitrary partial or total volume of a continuous solid material in an initial state which we denote as reference configuration. Since in the case of homogeneous isotropic fluids without memory effects, particles can be rearranged freely, there is no particular configuration which could be used as representative initial state. The following derivations with respect to deformations are therefore not directly applicable for fluids.

It is important to note that the reference configuration can be chosen arbitrarily. The body (or part thereof) is in particular not necessarily in a stress-free state, in fact, a solid body needs not even to have a stress-free configuration. We define a Cartesian coordinate system such that every point P (location $\hat{\mathbf{r}}$) of the body is associated with coordinates X, Y, Z whereby capital letters and hat over the vector symbol are used to denote the reference configuration (a generalization to other rectangular coordinate systems is performed later)

$$P : \hat{\mathbf{r}} = \begin{bmatrix} X \\ Y \\ Z \end{bmatrix} = (X, Y, Z)^{\mathsf{T}}.$$

Like in Chapter 2, a mathematically imprecise, but convenient abbreviated notation is used and vectors as well as tensors and their matrix representation of components are not distinguished.

Let Q with position vector $\hat{\mathbf{r}} + d\hat{\mathbf{r}}$ be a second point, located at an infinitesimal distance, $d\hat{\mathbf{r}} = (dX, dY, dZ)$, from P :

$$Q : \hat{\mathbf{r}} + d\hat{\mathbf{r}} = \begin{bmatrix} X + dX \\ Y + dY \\ Z + dZ \end{bmatrix}.$$

After some displacement and deformation, the (material) points P, Q are located at new (spatial) positions P', Q' with associated position vectors (Fig. 3.1).

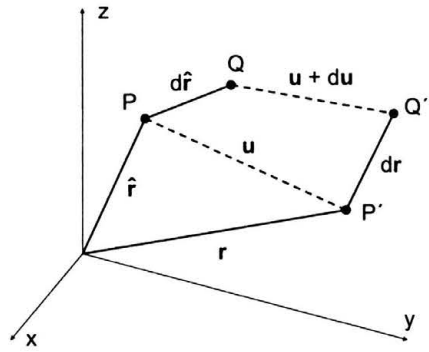

FIGURE 3.1. Definition of displacement vector $\mathbf{u}$

$$P' : \hat{\mathbf{r}} + \mathbf{u} = \begin{bmatrix} X + u_x \\ Y + u_y \\ Z + u_z \end{bmatrix} = \mathbf{r}(X, Y, Z) = \begin{bmatrix} x(X, Y, Z) \\ y(X, Y, Z) \\ z(X, Y, Z) \end{bmatrix}$$

and

$$Q' : \hat{\mathbf{r}} + d\hat{\mathbf{r}} + \mathbf{u} + d\mathbf{u} = \begin{bmatrix} X + dX + u_x + du_x \\ Y + dY + u_y + du_y \\ X + dZ + u_z + du_z \end{bmatrix} = \mathbf{r} + d\mathbf{r} = \begin{bmatrix} x + dx \\ y + dy \\ z + dz \end{bmatrix} \text{ respectively.}$$

$\mathbf{u}(X, Y, Z) = [u_x(X, Y, Z), u_y(X, Y, Z), u_z(X, Y, Z)]^{\mathsf{T}}$ is denoted as displacement vector and lower case letters are used to refer to actual positions. Since $\mathbf{r} = \hat{\mathbf{r}} + \mathbf{u}$, $d\mathbf{r}$ can be written as

$$d\mathbf{r} = \begin{bmatrix} dx \\ dy \\ dz \end{bmatrix}, \quad \text{whereby}$$

$$dx = \left(\frac{\partial x}{\partial X}\right) dX + \left(\frac{\partial x}{\partial Y}\right) dY + \left(\frac{\partial x}{\partial Z}\right) dZ$$

$$= dX + du_x = \left(1 + \left(\frac{\partial u_x}{\partial X}\right)\right) dX + \left(\frac{\partial u_x}{\partial Y}\right) dY + \left(\frac{\partial u_x}{\partial Z}\right) dZ,$$

$$dy = \ldots$$

$$dz = \ldots$$

dy and dz are obtained by cyclic permutation. Accordingly,

$$d\mathbf{r} = (\mathbf{1} + \mathbf{J}) d\hat{\mathbf{r}} = \mathbf{F}\, d\hat{\mathbf{r}}.$$

The displacement gradient $\mathbf{J}$ is defined as

$$\mathbf{J} = \begin{bmatrix} \frac{\partial u_x}{\partial X} & \frac{\partial u_x}{\partial Y} & \frac{\partial u_x}{\partial Z} \\ \frac{\partial u_y}{\partial X} & \frac{\partial u_y}{\partial Y} & \frac{\partial u_y}{\partial Z} \\ \frac{\partial u_z}{\partial X} & \frac{\partial u_z}{\partial Y} & \frac{\partial u_z}{\partial Z} \end{bmatrix} \tag{3.1}$$

whereas $\mathbf{F} = \mathbf{1} + \mathbf{J}$ is referred to as the deformation gradient.

In order to obtain a measure for the local strain resulting from a deformation of the body, we calculate the length of $d\hat{\mathbf{r}}$ in the deformed state $(d\mathbf{r})$:

$$|d\mathbf{r}|^2 = (d\mathbf{r}, d\mathbf{r}) = d\mathbf{r}^2 = [dx, dy, dz] \cdot \begin{bmatrix} dx \\ dy \\ dz \end{bmatrix} = (d\mathbf{r})^{\mathsf{T}} d\mathbf{r}.$$

The change in length is given by

$$dr^2 - dR^2 = (d\hat{\mathbf{r}})^{\mathsf{T}} (\mathbf{1} + \mathbf{J}^{\mathsf{T}})(\mathbf{1} + \mathbf{J}) d\hat{\mathbf{r}} - dR^2$$
$$= (d\hat{\mathbf{r}})^{\mathsf{T}} (\mathbf{J}^{\mathsf{T}} + \mathbf{J} + \mathbf{J}\mathbf{J}^{\mathsf{T}}) d\hat{\mathbf{r}} = (d\hat{\mathbf{r}})^{\mathsf{T}} (\mathbf{F}^{\mathsf{T}}\mathbf{F} - \mathbf{1}) d\hat{\mathbf{r}} \tag{3.2}$$

whereby it is again noted that the reference configuration may already have internal strains.

Note: In case of small deformations and in the absence of rigid displacements, the nonlinear term $\mathbf{J}^{\mathsf{T}}\mathbf{J}$ *can be neglected and the engineering strain tensor is obtained*

$$\frac{1}{2}(\mathbf{J}^{\mathsf{T}} + \mathbf{J}) = \begin{bmatrix} \frac{\partial u_x}{\partial X} & \frac{1}{2}\left(\frac{\partial u_x}{\partial Y} + \frac{\partial u_y}{\partial X}\right) & \frac{1}{2}\left(\frac{\partial u_x}{\partial Z} + \frac{\partial u_z}{\partial X}\right) \\ \frac{1}{2}\left(\frac{\partial u_y}{\partial X} + \frac{\partial u_x}{\partial Y}\right) & \frac{\partial u_y}{\partial Y} & \frac{1}{2}\left(\frac{\partial u_y}{\partial Z} + \frac{\partial u_z}{\partial Y}\right) \\ \frac{1}{2}\left(\frac{\partial u_z}{\partial X} + \frac{\partial u_x}{\partial Z}\right) & \frac{1}{2}\left(\frac{\partial u_z}{\partial Y} + \frac{\partial u_y}{\partial Z}\right) & \frac{\partial u_z}{\partial Z} \end{bmatrix}. \tag{3.3}$$

The factor $1/2$ *derives from the expansion of the square root, if the actual length, and not the length squared, is calculated.*

From (3.2) is seen, that the quantity

$$\mathbf{E} = \frac{1}{2}(\mathbf{F}^{\mathsf{T}}\mathbf{F} - \mathbf{1}) \tag{3.4}$$

which is denoted as Green-Lagrange tensor describes strain also in case of large deformations. In addition, the right Cauchy-Green deformation tensor,

$$\mathbf{C} = \mathbf{F}^{\mathsf{T}}\mathbf{F} \tag{3.5}$$

is often used in constitutive equations.

3.2. Forces: Stress

While the previous paragraph is related primarily to solids, the concept of stress applies equally for fluids or solids. We consider the interior of a fluid or solid continuum, in particular an element of a (virtual) interior surface, in a deformed and/or displaced state, $df = dy\,dz$. The outer normal (unit vector $\mathbf{n}$) of this element has x-direction. The element of force, $d\hat{\mathbf{p}}$, which the adjacent material exerts on df is written as $d\hat{\mathbf{p}} = \mathbf{p}df$ with the aid of the stress vector $\mathbf{p}$ (force per unit area); $\mathbf{p}$ is decomposed into the three components

$$\sigma_{xx} = \sigma_x \quad \text{normal stress,}$$
$$\tau_{xy},\ \tau_{xz} \quad \text{shear stresses}$$

whereby the indices are chosen such that the first index denotes the outer normal of the surface element under consideration while the second index indicates the direction of the component (Fig. 3.2).

Upon application of the same procedure to the other coordinate directions, an ensemble of components is obtained as

$$\boldsymbol{\sigma} = \begin{bmatrix} \sigma_x & \tau_{xy} & \tau_{xz} \\ \tau_{yx} & \sigma_y & \tau_{yz} \\ \tau_{zx} & \tau_{zy} & \sigma_z \end{bmatrix}$$

which is denoted as Cauchy stress tensor (Fig. 3.3). That this has in fact the properties of a tensor is seen when the particular coordinate system (x, y, z) is subjected to a rotation; it will be seen that $\boldsymbol{\sigma}$ then transforms as

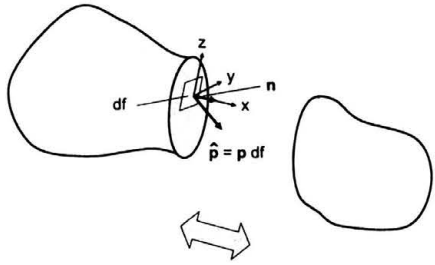

FIGURE 3.2. Interior surface of a body, virtually cut into two pieces. The vector $\mathbf{p}df$ denotes the force acting on the surface element df which is exerted by the connecting surface (in order to keep the state of deformation, the internal forces acting along the virtual cut have to be applied). $\mathbf{n}, (|\mathbf{n}| = 1)$ is the outer normal of df.

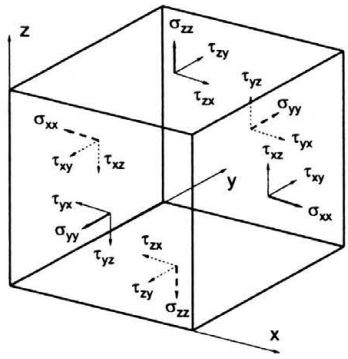

FIGURE 3.3. Definition of the components of the stress tensor

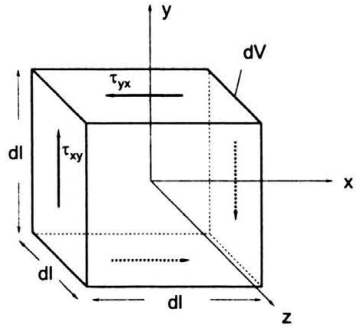

FIGURE 3.4. Momentum balance around $z-$ axis. The other stress components acting on the cube do not contribute to the moment around this axis.

$\boldsymbol{\sigma}' = \mathbf{D}^{-1} \cdot \boldsymbol{\sigma} \cdot \mathbf{D}$. The stress tensor is furthermore symmetric. This follows from angular equilibrium (Fig. 3.4): The moment acting with respect to the center of mass of the cube around the z-axis is due to the shear stresses τ_{xy} and τ_{yx} only and is proportional to the edge length $(\mathrm{dl})^3$, because the forces are proportional to $(\mathrm{dl})^2$ and the moment arm to $(\mathrm{dl})^1$, while the moment of inertia is proportional to $(\mathrm{dl})^5$ because the mass is proportional to $(\mathrm{dl})^3$ and the radius of inertia to $(\mathrm{dl})^2$. If the moment would not be zero i.e. $\tau_{xy} \neq \tau_{yx}$, there would be infinite rotational accelerations as $\mathrm{dl} \to 0$. The same holds for the other axes, accordingly, the tensor has to be symmetric.

An element of surface area with an arbitrary spatial orientation is now considered (Fig. 3.5),

$$d\mathbf{f} = [df_x, df_y, df_z] = \mathbf{n}df = [n_x df, n_y df, n_z df] .$$

The forces acting on the infinitesimal tetraeder have to be in equilibrium, because the forces are proportional to $(dl)^2$ while its mass is proportional to $(dl)^3$. If the forces were not in equilibrium, the tetraeder would experience an infinite acceleration as $dl \to 0$. Accordingly,

$$\begin{aligned}
\sigma_x n_x df + \tau_{yx} n_y df + \tau_{zx} n_z df &= p_x df, \\
\tau_{xy} n_x df + \sigma_y n_y df + \tau_{zy} n_z df &= p_y df, \\
\tau_{xz} n_x df + \tau_{yz} n_y df + \sigma_z n_z df &= p_z df,
\end{aligned}$$

or

$$d\mathbf{p} = \boldsymbol{\sigma} \cdot \mathbf{n}df \tag{3.6}$$

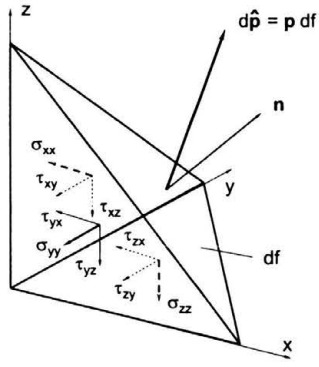

FIGURE 3.5. Equilibrium of an infinitesimal tetraeder. The unit vector $\mathbf{n}$ denotes the outer normal to the surface element df

where the dot is used to denote a scalar product.

Note: Upon application of a transformation $\mathbf{D}$ *to Eq.* (3.6), *one obtains*

$$\mathbf{D} \cdot d\mathbf{p} = \mathbf{D} \cdot \boldsymbol{\sigma} \cdot \mathbf{n}df = \mathbf{D} \cdot \boldsymbol{\sigma} \cdot \mathbf{D}^{-1} \cdot \mathbf{D} \cdot \mathbf{n}df$$

which shows that $\boldsymbol{\sigma}$ *transforms as a tensor.*

From now on, solids and fluids have to be treated separately.

Solids

The Cauchy stress tensor is always related to a surface element in the deformed state. In case of large deformations, however, a surface element given in a specific state of deformation changes its shape and size as the deformation process continues such that the Cauchy stress tensor is defined with respect to a different surface element after each deformation step. A consistent procedure is reached, if the stress tensor is always related to a surface element in the reference configuration which can be made in the following fashion. The quantity $\mathbf{a} \cdot (\mathbf{b} \times \mathbf{c})$ is equal to the volume of a body formed by the arbitrary vectors $\mathbf{a}, \mathbf{b}, \mathbf{c}$ (not collinear). For every matrix $\mathbf{M}$ whose determinant is not zero, the theorem holds (from linear algebra, the formula is related to the volume of a parallelepiped with edges $\mathbf{a}, \mathbf{b}, \mathbf{c}$):

$$\mathbf{Ma} \cdot (\mathbf{Mb} \cdot \mathbf{Mc}) = \det(\mathbf{M})\, \mathbf{a} \cdot (\mathbf{b} \times \mathbf{c}).$$

From this follows

$$d\mathbf{f}\,(\text{actual configuration}) = \det(\mathbf{F})\, \mathbf{F}^{-\mathsf{T}} d\hat{\mathbf{f}}\,(\text{reference configuration}).$$

Upon application of this relation to the Cauchy stress tensor, one finds that

$$\mathbf{P} = \det(\mathbf{F})\, \boldsymbol{\sigma} \mathbf{F}^{-\mathsf{T}} \tag{3.7}$$

which is denoted as nominal or first Piola-Kirchhoff stress tensor (in general non-symmetric!). It relates the stresses in the actual configuration to the equivalent surface element in the reference configuration. It is convenient to express also the stresses with respect to the reference configuration, which can be achieved by multiplication with $\mathbf{F}^{-1}$

$$\mathbf{T} = \det(\mathbf{F})\, \mathbf{F}^{-1} \boldsymbol{\sigma} \mathbf{F}^{-\mathsf{T}}. \tag{3.8}$$

This is a useful formulation to describe stresses under large deformations; $\mathbf{T}$ is called the 2^{nd} Piola-Kirchhoff stress tensor which is again symmetric, but has no direct physical interpretation.

Fluids

Homogeneous isotropic fluids have no reference configuration; accordingly, stresses occur only when internal friction effects due to gradients in flow fields are present. In particular, only the momentary state of flow is of importance (fluids with memory effects, like liquid crystals, are not considered here). This will be considered in the next paragraph.

3.3. Constitutive Equations

The mechanical properties of a solid or fluid body with respect to deformability are introduced by way of the constitutive equation which relates the state of deformation (or its derivative with respect to time) to the stress state. Solids and fluids have to be treated differently.

Solids

There are numerous ways to describe the constitutive behavior of the existing vast variety of solid materials which can be found in the literature on continuum mechanics. A straightforward method to formulate a constitutive equation which is useful for large-deformation and nonlinear cases consists of the choice of an appropriate scalar function W which describes the elastic strain energy density (hyperelastic material). A scalar function is invariant under transformations, therefore, the isotropy group of the material (isotropic, orthotropic, etc.) can easily be integrated. Dissipative effects (internal friction) are thereby not included, however.

In order to arrive at a formulation which is valid for nonlinear and large-deformation problems, the 2nd Piola-Kirchhoff stress tensor has to be used which is obtained according to

$$T_{ij} = 2\frac{\partial W}{\partial C_{ij}} \tag{3.9}$$

For a derivation of the relation (3.9) which is based on the fact that the 2nd Piola-Kirchhoff stress tensor and the Cauchy-Green deformation tensor are connected in the sense that the work per unit of time performed by the stresses equals $\sum_{i,j} (\mathbf{T})_{ij} \cdot (\dot{\mathbf{C}})_{ij}$ see e.g. [1]. Since W is invariant, it has to be a function of the invariants I_i associated with $\mathbf{C}$. The number of invariants thereby depends on the isotropy group of the material under consideration: 3 for isotropic, 5 for transversely anisotropic, etc.

For isotropic materials, the invariants are

$$\begin{aligned} I_1 &= \mathrm{tr}\mathbf{C}, \\ I_2 &= \frac{1}{2}\left((\mathrm{tr}\mathbf{C})^2 - \mathrm{tr}\mathbf{C}^2\right), \\ I_3 &= \det \mathbf{C}. \end{aligned}$$

For Veronda-Westmann materials, e.g., the expression is

$$\begin{aligned} W &= \alpha_1\left(\mathrm{e}^{\alpha_2(I_1-3)} - 1\right) + \alpha_3\,(I_2 - 3)\,, \\ I_3 &= 1 \quad \text{(incompressibility)}\,. \end{aligned} \tag{3.10}$$

Here α_1, α_2, α_3 are constants which have to be fitted to experimental measurements. Figure 3.6 shows the application of this expression to uterine tissue of a rabbit in uniaxial tension.

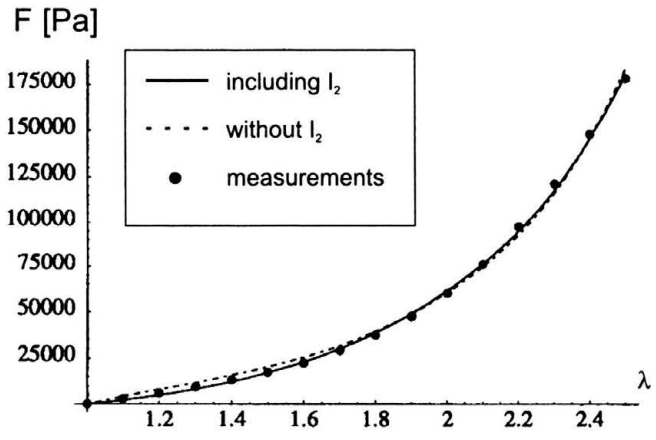

FIGURE 3.6. Veronda Westmann model (force F as function of the stretch ratio $\lambda = I/I_0$, i.e. the relation of the actual length to the original length of a strip of material) fitted to rabbit uterine tissue in uniaxial elongation. Measurements are adopted from [2].

In case of transverse anisotropy (direction $\mathbf{n}$, $|\mathbf{n}| = 1$), two further invariants are introduced

$$\begin{aligned} I_4 &= \mathbf{n} \cdot \mathbf{C} \cdot \mathbf{n}, \\ I_5 &= \mathbf{n} \cdot \mathbf{C}^2 \cdot \mathbf{n}. \end{aligned}$$

Viscoelastic damping can be taken into account by including a hereditary integral over the past history of the deformation tensor or its derivative with respect to time (this is not straightforward, however, and the reader is referred to the literature).

Fluids

The stress state in an ideal, inviscid, isotropic and incompressible fluid is described by an isotropic tensor which is invariant under transformations (such that no shear stresses occur). Such a tensor has the general form (the minus sign is by definition)

$$\boldsymbol{\sigma} = \begin{bmatrix} -p & 0 & 0 \\ 0 & -p & 0 \\ 0 & 0 & -p \end{bmatrix} \tag{3.11}$$

and describes a hydrostatic pressure state.

In case of an incompressible viscous fluid, stresses in addition to the hydrostatic pressure develop because of internal friction effects which become effective as soon as the flow field is such that fluid particles execute relative shearing motions. Accordingly, the gradient of the flow field, $\mathbf{v}(\mathbf{r}, t)$ has to be considered. Since derivatives involve infinitesimal changes of the momentary configuration, the time derivative of the engineering strain tensor (3.3), disregarding large displacement and deformation effects, can be used to formulate a constitutive law. In the simplest case, the stress tensor and the velocity gradient are proportional:

$$\begin{aligned} \boldsymbol{\sigma} &= 2\eta \nabla \mathbf{v} \\ &= 2\eta \begin{bmatrix} \frac{\partial v_x}{\partial x} & \frac{1}{2}\left(\frac{\partial v_x}{\partial y} + \frac{\partial v_y}{\partial x}\right) & \frac{1}{2}\left(\frac{\partial v_x}{\partial z} + \frac{\partial v_z}{\partial x}\right) \\ \frac{1}{2}\left(\frac{\partial v_y}{\partial x} + \frac{\partial v_x}{\partial y}\right) & \frac{\partial v_y}{\partial y} & \frac{1}{2}\left(\frac{\partial v_y}{\partial z} + \frac{\partial v_z}{\partial y}\right) \\ \frac{1}{2}\left(\frac{\partial v_z}{\partial x} + \frac{\partial v_x}{\partial z}\right) & \frac{1}{2}\left(\frac{\partial v_z}{\partial y} + \frac{\partial v_y}{\partial z}\right) & \frac{\partial v_z}{\partial z} \end{bmatrix} \end{aligned} \tag{3.12}$$

The proportionality factor η is denoted as viscosity and fluids which obey this law are called Newtonian fluids. Non-Newtonian fluids, such as, e.g. blood under flow conditions which include locations with vanishing shear components over extended periods of time may involve nonlinear expressions in the velocity gradient. In case of an incompressible Newtonian fluid, stresses according to Eqs. (3.11) and (3.12) are added in that the stepwise procedure

applied here can be regarded as part of a power expansion in the velocity gradient.

3.4. Equations of Motion

We consider a deformable body (volume V) under the influence of forces (Fig. 3.7). We thereby distinguish two types of forces, viz., field forces acting on the entire body such as gravity or electromagnetic forces and forces acting on the surface F such as forces due to contacts. Momentum balance then requires

$$\frac{d}{dt}\int_V (\rho \mathbf{v})\, dV = \int_V \rho \mathbf{k} dV + \oint_F \boldsymbol{\sigma} \cdot \mathbf{n} dF. \tag{3.13}$$

In this equation, ρ denotes the density of the material, $\mathbf{v}$ the velocity field, $\mathbf{k}$ the field force per mass, $\boldsymbol{\sigma}$ the Cauchy stress tensor and $\mathbf{n}$ the outer normal. Using Gauss' theorem, the last term in Eq. (3.13) can be converted into a volume integral,

$$\oint_F \boldsymbol{\sigma} \cdot \mathbf{n} dF = \int_V \mathrm{div}\boldsymbol{\sigma} dV.$$

Since the momentum balance has to be fulfilled for any volume, it follows

$$\frac{d(\rho \mathbf{v})}{dt} = \rho \mathbf{k} + \mathrm{div}\boldsymbol{\sigma}. \tag{3.14}$$

In this form, the equation is written in what is called the "Lagrangian" formulation which implies that the time derivative is total and follows the material. When soft particle methods (see later) are used for numerical solution

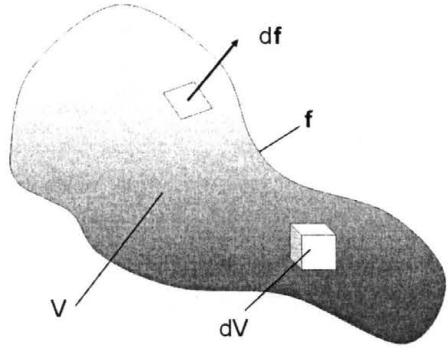

FIGURE 3.7. Volume V with surface f, volume element dV, surface element $d\mathbf{f} = \mathbf{n}df$

purposes, the Lagrangian form of the equation is often applied. It can be converted into the "Eulerian" form by introducing partial derivatives:

$$\frac{\partial(\rho\mathbf{v})}{\partial t} + (\mathbf{v}\cdot\boldsymbol{\nabla})(\rho\mathbf{v}) = \rho\mathbf{k} + \mathrm{div}\boldsymbol{\sigma}. \tag{3.15}$$

For solids, this equation is worked out with the constitutive equation of choice, accordingly, a wide variety of equations can be found throughout the literature. While the velocity field $\mathbf{v}(\mathbf{r},t)$ can readily be related to the displacements $\mathbf{u}$, the stresses $\boldsymbol{\sigma}$ have to be expressed in the same variables with the aid of the constitutive relation.

In case of incompressible Newtonian fluids, the equation of motion is in contrast well defined and is therefore treated in more detail in the following. Inserting (3.11) and (3.12) into Eq. (3.15) yields the Navier-Stokes equation

$$\rho\frac{\partial\mathbf{v}}{\partial t} + \rho(\mathbf{v}\cdot\boldsymbol{\nabla})\mathbf{v} = \rho\mathbf{k} - \boldsymbol{\nabla}p + \eta\nabla^2\mathbf{v}. \tag{3.16}$$

Incompressibility requires furthermore

$$\boldsymbol{\nabla}\cdot\mathbf{v} = 0. \tag{3.17}$$

This equation is obtained by balancing the in- and outflow of a volume element dV (see later).

Note: If the last term in Eq. (3.16) *is dropped, i.e. only* (3.11) *is used (inviscid fluid), a set of equations called Euler equations is obtained.*

In Eqs. (3.15) and (3.16) is seen that the velocity field $\mathbf{v}(\mathbf{r},t)$ which usually is to be calculated appears in nonlinear form. This often prevents analytic solutions. Numerical procedures have to be applied most often.

Since every partial volume of a continuum has an infinite number of degrees of freedom, equations of continuum mechanics (fluid or solid) are scalable as a rule. This is demonstrated in the following with Eq. (3.16) for stationary flow and without the $\rho\mathbf{k}$ term. If in the equation

$$\rho(\mathbf{v}\cdot\boldsymbol{\nabla})\mathbf{v} = -\boldsymbol{\nabla}p + \eta\nabla^2\mathbf{v}$$

the dimensionless quantities are introduced: $\hat{\mathbf{u}} = \mathbf{v}/V$, $\hat{\mathbf{r}} = \mathbf{r}/D$, $P = pD/V\eta$ whereby V and D are in essence arbitrarily chosen quantities which are characteristic for the problem under investigation (e.g. the diameter of a tube, the

flow velocity far away from the object under consideration), a dimensionless equation is obtained

$$\frac{\rho V D}{\eta}\left(\hat{\mathbf{u}}\cdot\boldsymbol{\nabla}\right)\hat{\mathbf{u}} = -\boldsymbol{\nabla}P + \nabla^2\hat{\mathbf{u}}.$$

The (dimensionless) parameter $\rho VD/\eta$, called Reynolds number, is a scaling factor and characterizes the relation between inertial and viscous forces. Turbulence is observed when the Reynolds number exceeds some critical value which implies that the inertial forces dominate over the viscous damping forces. Problems having the same Reynolds number exhibit similar flow characteristics. Other scaling factors can be defined for other continuum mechanics' problems. A further such scaling quantity will be introduced in the next paragraph.

Many convective transport conduits in biology are long and cylindrical where axial flow prevails (blood vessels, lymph vessels, urethra, etc.). Cylindrical coordinates are more useful to describe such systems than Cartesian coordinates. Cylindrical coordinates (Fig. 3.8) are orthogonal but curvilinear which has to be taken into account when derivatives are used.

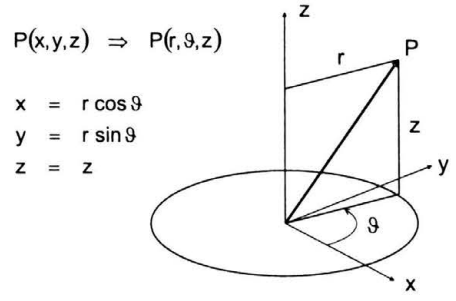

FIGURE 3.8. Cylindrical coordinates

We consider a general transformation of a set of Cartesian coordinates x_1, x_2, x_3 into a curvilinear, orthogonal system ξ_1, ξ_2, ξ_3 by way of the functions

$$\begin{aligned} x_1 &= x_1\left(\xi_1,\xi_2,\xi_3\right), \\ x_2 &= x_2\left(\xi_1,\xi_2,\xi_3\right), \\ x_3 &= x_3\left(\xi_1,\xi_2,\xi_3\right). \end{aligned} \tag{3.18}$$

The rectangular base which is associated with the new system is defined by way of

$$\mathbf{e}_{\xi_i} = \frac{\partial\mathbf{r}}{\partial\xi_i}\left|\frac{\partial\mathbf{r}}{\partial\xi_i}\right|^{-1} = h_i\frac{\partial\mathbf{r}}{\partial\xi_i},$$

$\mathbf{r} = x_1\mathbf{e}_{x_1} + x_2\mathbf{e}_{x_2} + x_3\mathbf{e}_{x_3}$ is a position vector beginning at the origin. With

$$d\mathbf{r} = \sum_{i=1,2,3} \frac{\partial \mathbf{r}}{\partial \xi_i} d\xi_i$$

one finds for the line element, using (3.18)

$$\begin{aligned} ds^2 = (d\mathbf{r} \cdot d\mathbf{r}) &= \sum_{i=1,2,3} h_i^2 d\xi_i^2, \\ d\mathbf{r} &= h_1 d\xi_1 \mathbf{e}_1 + h_2 d\xi_2 \mathbf{e}_2 + h_3 d\xi_3 \mathbf{e}_3, \end{aligned} \tag{3.19}$$

with

$$h_i^2 = \sum_{j=1,2,3} \left(\frac{\partial x_j}{\partial \xi_i} \right)^2 . \tag{3.20}$$

In case of cylindrical coordinates,

$$d\mathbf{r} = dr\mathbf{e}_r + rd\vartheta \mathbf{e}_\vartheta + dz\mathbf{e}_z, \quad h_1 = h_3 = 1, \quad h_2 = r.$$

The differentiation operators ∇, ∇^2 applied to a scalar field, can be written, e.g. in cylindrical coordinates using Eqs. (3.19) and (3.20)

$$\begin{aligned} \nabla \ldots &= \left(\frac{\partial \ldots}{\partial r}, \frac{1}{r} \frac{\partial \ldots}{\partial \vartheta}, \frac{\partial \ldots}{\partial z} \right), \\ \nabla^2 \ldots &= \frac{1}{r} \frac{\partial}{\partial r} \left(r \frac{\partial \ldots}{\partial r} \right) + \frac{1}{r^2} \frac{\partial^2 \ldots}{\partial \vartheta^2} + \frac{\partial^2 \ldots}{\partial z^2}. \end{aligned} \tag{3.21}$$

The derivation of the the continuity equation $\operatorname{div} \mathbf{v} = \nabla \cdot \mathbf{v} = 0$ in cylindrical coordinates proceeds as follows:

The inflow—outflow balance for coordinate ξ_2 reads (cf. Fig. 3.9),

$$\begin{aligned} v_{\xi_2}(\xi_1, \xi_2, \xi_3)\, h_1 d\xi_1 h_3 d\xi_3 - v_{\xi_2}(\xi_1, \xi_2 + d\xi_2, d\xi_3)\, h_1 d_{\xi_1} h_3 d\xi_3 \\ = -\frac{\partial \left[v_{\xi_2}(\xi_1, \xi_2, \xi_3)\, h_1 d\xi_1 h_3 d\xi_3 \right]}{\partial \xi_2} d\xi_2. \end{aligned}$$

Per unit of volume, on including all three coordinates, one obtains

$$\begin{aligned} &\frac{1}{h_1 h_2 h_3 d\xi_1 d\xi_2 d\xi_3} \left(\frac{\partial}{\partial_{\xi_1}} (v_{\xi_1} h_2 d_{\xi_2} h_3 d_{\xi_3}) + \frac{\partial}{\partial_{\xi_2}} (v_{\xi_2} h_1 d_{\xi_1} h_3 d_{\xi_3}) \right. \\ &\qquad \left. + \frac{\partial}{\partial_{\xi_3}} (v_{\xi_3} h_1 d_{\xi_1} h_2 d_{\xi_2}) \right) = \\ &\frac{1}{h_1 h_2 h_3} \left(\frac{\partial}{\partial \xi_1} (v_{\xi_1} h_2 h_3) + \frac{\partial}{\partial \xi_2} (v_{\xi_2} h_1 h_3) + \frac{\partial}{\partial \xi_3} (v_{\xi_3} h_1 h_2) \right) = \operatorname{div} \mathbf{v}. \end{aligned}$$

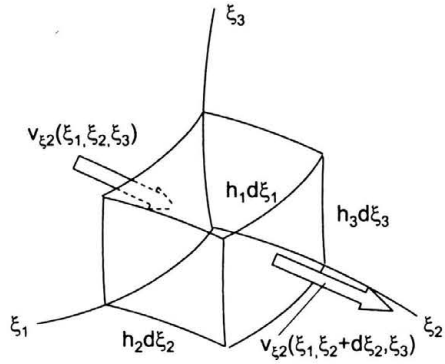

FIGURE 3.9. Derivation of the continuity equation $\operatorname{div}\mathbf{v} = \boldsymbol{\nabla}\cdot\mathbf{v} = 0$ in cylindrical coordinates

In case of vector fields, e.g. $\mathbf{v}(\mathbf{r},t) = v_r\mathbf{e}_r + v_\vartheta\mathbf{e}_\vartheta + v_z\mathbf{e}_z$ the operators have to be applied to the base vectors also (Fig. 3.10). Using

$$\begin{aligned}
&\frac{\partial\mathbf{e}_r}{\partial r} = 0, \quad \frac{\partial\mathbf{e}_r}{\partial\vartheta} = \mathbf{e}_\vartheta, \quad \frac{\partial\mathbf{e}_r}{\partial z} = 0\\
&\frac{\partial\mathbf{e}_\vartheta}{\partial r} = 0, \quad \frac{\partial\mathbf{e}_\vartheta}{\partial\vartheta} = -\mathbf{e}_r, \quad \frac{\partial\mathbf{e}_\vartheta}{\partial z} = 0\\
&\frac{\partial\mathbf{e}_z}{\partial z} = \frac{\partial\mathbf{e}_\vartheta}{\partial z} = \frac{\partial\mathbf{e}_z}{\partial z} = 0,
\end{aligned} \tag{3.22}$$

one finds, after some calculation, the Navier-Stokes equation in cylindrical coordinates

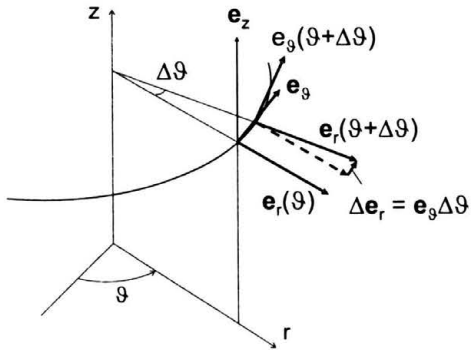

FIGURE 3.10. Derivatives of base vectors in case of cylindrical coordinates

$$\rho\left[\frac{\partial v_r}{\partial t}+(\mathbf{v}\cdot\operatorname{grad}v_r)-\frac{v_\vartheta^2}{r}\right]=-\frac{\partial p}{\partial r}+\eta\left[\nabla^2 v_r-\frac{v_r}{r^2}-\frac{2}{r^2}\frac{\partial v_\vartheta}{\partial\vartheta}\right],$$

$$\rho\left[\frac{\partial v_\vartheta}{\partial t}+(\mathbf{v}\cdot\operatorname{grad}v_\vartheta)-\frac{v_\vartheta^{v_r}}{r}\right]=\frac{1}{r}\frac{\partial p}{\partial\vartheta}+\eta\left[\nabla^2 v_\vartheta-\frac{v_\vartheta}{r^2}-\frac{2}{r^2}\frac{\partial v_r}{\partial\vartheta}\right], \quad (3.23)$$

$$\rho\left[\frac{\partial v_z}{\partial t}+(\mathbf{v}\cdot\operatorname{grad}v_z)\right]=-\frac{\partial p}{\partial z}+\eta\nabla^2 v_z,$$

along with the equation of continuity

$$\frac{1}{r}\frac{\partial}{\partial r}(rv_r)+\frac{1}{r}\frac{\partial v_\vartheta}{\partial\vartheta}+\frac{\partial v_z}{\partial z}. \quad (3.24)$$

3.5. Analytic Solutions of the Navier-Stokes Equation which Are of Use in Biomechanics

In contrast to solids, where an enormous diversity of continuum mechanical equations can be derived, the Navier-Stokes equations are quite universal (also non-Newtonian fluids can be modeled) and are often used in biomechanics.

Due to their quasilinear nature (the second order term is involved in a first order derivative only) the Navier-Stokes equations have however only a few analytical solutions. Some of them are of importance in biomechanics (mostly tube flow) and are presented in the following.

3.5.1. Hagen-Poiseuille flow

The well known Hagen-Poiseuille flow is obtained when one-dimensional, stationary, laminar flow of an incompressible Newtonian fluid in an infinite straight and rigid circular tube is assumed. With $v_r = v_\vartheta = \partial v_i/\partial t = 0$ $(i = r, \theta, z)$ the four Eqs. (3.23), (3.24) reduce to

$$\frac{\partial p}{\partial r}=\frac{\partial p}{\partial\vartheta}=0 \quad \text{and} \quad \frac{d^2 v_z}{dr^2}+\frac{1}{r}\frac{dv_z}{dr}=\frac{1}{\eta}\frac{dp}{dz}. \quad (3.25)$$

Since the problem is invariant with respect to tranlations, the pressure gradient, $dp/dz = p_z$ is constant and represents an inhomogeneity for the (ordinary) differential Equation (3.25).

Note: From the equation of continuity (3.24) *follows under the conditions considered here* $\partial v_z/\partial z = 0$ *which implies that the nonlinear (often called*

convective) acceleration term disappears. This is always the case in straight, parallel flow. The equations then become linear (and solvable), and in fact all cases considered in the following have this property (except sect. 3.5.3.).

With the usual procedure for inhomogeneous equations (add a particular solution of the inhomogeneous equation to the general solution of the homogeneous equation, then apply the boundary conditions $v_z(r = R) = 0$, $v_z(r = 0) < \infty$) the Hagen-Poiseuille formula is found (parabolic velocity profile)

$$v_z = \frac{(-p_z) R^2}{4\eta} \left(1 - \frac{r^2}{R^2}\right) \tag{3.26}$$

with the total flow (integrated over the cross section) $Q = (-p_z) R^4 / (8\eta)$.

3.5.2. Witzig-Womersley flow

We assume the same geometrical and axial flow conditions as above, but the pressure gradient is now assumed to vary harmonically in time, $dp/dz = p_z^0 \exp(i\omega t)$ (since the equations are linear, the solution for an arbitrary time dependence of the pressure gradient can be obtained by Fourier superposition). With the separation ansatz $v_z(r, t) = v(r) \exp(i\omega t)$ the equation

$$\frac{d^2 v}{dr^2} + \frac{1}{r}\frac{dv}{dr} - \frac{i\rho\omega}{\eta} v = \frac{1}{\eta} p_z^0 \tag{3.27}$$

is obtained. Upon application of the transformation $\zeta^2 = i^3 \left(\omega\rho R^2/\eta\right)$ the homogeneous equation becomes a zero order Bessel equation

$$\frac{d^2 v}{d\zeta^2} + \frac{1}{\zeta}\frac{dv}{d\zeta} + v = 0. \tag{3.28}$$

With the (readily available) particular solution of the inhomogeneous equation and the same boundary conditions as above one arrives at

$$v_z(r, t) = \frac{-p_z^0}{i\rho\omega} \left(1 - \frac{J_0\left(i^{\frac{3}{2}} \alpha \frac{r}{R}\right)}{J_0\left(i^{\frac{3}{2}} \alpha\right)}\right) e^{i\omega t} \tag{3.29}$$

with the dimensionless Witzig-Womersley parameter $\alpha^2 = \omega\rho R^2/\eta$, see Fig. 3.11. (This solution was first presented by Konrad Witzig (1914) in his dissertation at the University of Berne, Switzerland). The Witzig-Womersley parameter, like the Reynolds number, characterizes the ratio of the inertial

forces to the viscous forces. While in stationary flow however the inertial forces are due to the convective contribution, in oscillating flow the inertial forces are due to the explicit time dependence and are dominant (often also in cases where the convective term in the Navier-Stokes equations does not disappear).

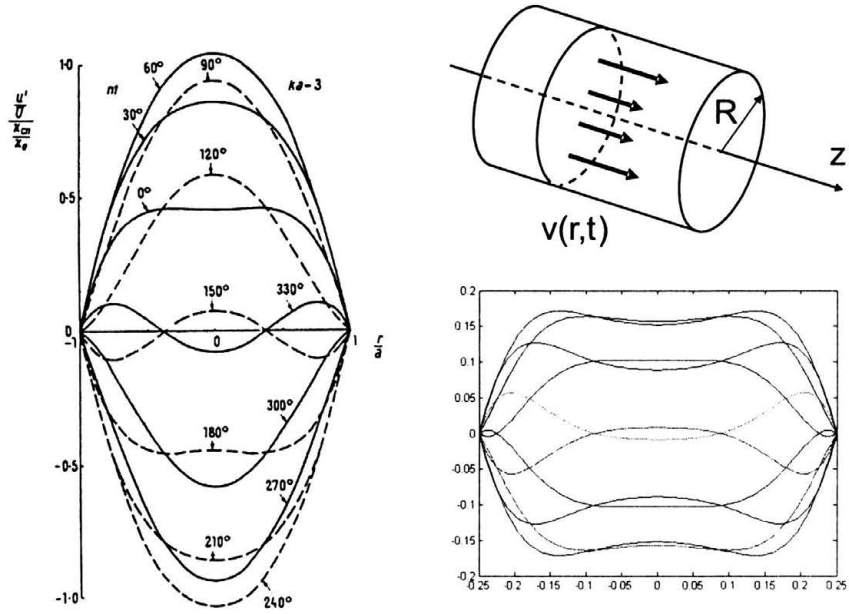

(a) (b)

FIGURE 3.11. Pulsatile flow in straight rigid tube, velocity profiles. (a) Original from Witzig's dissertation (University of Bern 1914), (b) Matlab simulation for $\alpha = 6.7$.

Since the tube is assumed as rigid, there is no pulse propagation (formally, the wave speed is infinite), in that all fluid particles along a stream line oscillate in phase. If a deformable tube is modeled, formulas for the wave speed can be obtained; however, only approximate solutions can be found.

Note: The Equation (3.29) *can readily be integrated over the cross section using theorems on Bessel functions to obtain the oscillating total flow. Furthermore, for* $\omega \to 0$, *Hagen Poiseuille flow should be obtained. That this is the case is seen from the power expansion of the zero order Bessel function*

$$J_0 = 1 + i\left(\frac{\alpha^2 r^2}{4R^2}\right) + \dots$$

when it is inserted into Eq. (3.29).

3.5.3. Couette Flow

This type of flow occurs generally in symmetrically rotating flow problems. A particular case is of importance, e.g., in viscosimeters of the form shown in Fig. 3.12. Such viscosimeters provide correct results for the (apparent) viscosity also in the case of non-Newtonian fluids. With the ansatz $\mathbf{v} = (0, v_\vartheta(r), 0)$, $p = p(r)$ and after making use of the continuity equation the two equations result (note that the convective term does not disappear)

$$\rho \frac{v^2}{r} = \frac{dp}{dr} \quad \text{and} \quad \frac{d^2v}{dr^2} + \frac{1}{r}\frac{dv}{dr} - \frac{v}{r^2} = 0. \tag{3.30}$$

With the boundary conditions $v(r = R_i) = 0$, $v(r = R_a) = \omega R_a$ the solution reads

$$v(r) = \frac{\omega R_a^2}{R_a^2 - R_i^2}\left(r - R_i^2 \frac{1}{r}\right) \tag{3.31}$$

from which the moment acting on the inner (rotating) cylinder

$$M = 4\pi\eta\omega R_a^2 R_i^2 \frac{1}{R_a^2 - R_i^2}$$

is obtained. This allows to determine the (effective) viscosity, i.e. the viscosity at the shear field given by ω also for non-Newtonian fluids, since the solution (3.31) is independent of the viscosity.

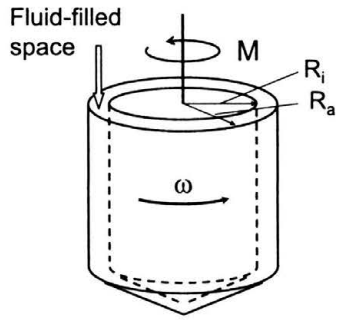

FIGURE 3.12. Special case of Couette flow, typical arrangement chosen for a viscosimeter. The inner cylinder is kept at a constant rotating speed; the necessary moment is monitored which allows to determine the viscosity of the fluid.

3.5.4. A laminar boundary layer

The concept of "boundary layers" was introduced by Ludwig Prandtl (1905) and reflects the fact that viscous effects are of particular influence in

the neighborhood of surfaces where velocity gradients are high. The simplest case of a laminar boundary layer (there are also turbulent boundary layers) is obtained when a Newtonian fluid over an oscillating plane is considered (Fig. 3.13). Cartesian coordinates are used here, and the plane is assumed to oscillate according to $\mathbf{v} = (v_0 \cos(\omega t), 0, 0)$. The solution is based on the ansatz $v_y = v_z = 0$, $v_x = v_x(y)$ only, furthermore, $\partial p/\partial x = 0$ since the problem is translationally invariant and the pressure is assumed to remain finite at infinity. The Navier-Stokes equations along with the equation of continuity yield

$$\frac{\partial p}{\partial y} = \frac{\partial p}{\partial z} = 0, \quad \text{and} \quad \rho \frac{\partial v_x}{\partial t} = \eta \frac{\partial^2 v_x}{\partial y^2}. \tag{3.32}$$

From the solution

$$v_x(y,t) = v_0 e^{-ky} \cos(\omega t - ky) \tag{3.33}$$

with $k^2 = \omega\rho/(2\eta)$ it is seen that at a distance of $\delta = \sqrt{2\eta/(\omega\rho)}$ the amplitude of the oscillation decays by a factor of $1/e$; δ is denoted as the thickness of the boundary layer.

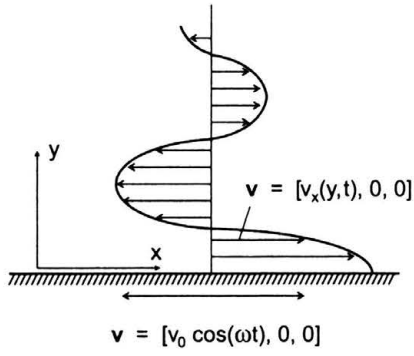

FIGURE 3.13. Example of a laminar boundary layer.

3.5.5. Hydraulic approximation

For many purposes in biological flow problems, simplified one-dimensional flow conditions, incompressibility and Newtonian viscosity properties can be assumed (e.g. arterial pulse propagation, lymph flow, flow in the urethra, tear channel). Instead of a velocity profile, only an average axial velocity is modeled. Such an approximation leads to what is called hydraulic approximation.

We start from the Navier-Stokes and continuity Eqs (3.23) and (3.24). Basic assumptions are $v_\vartheta = 0$, $v_r \ll v_z$. In the axial direction, the equation is treated as follows

$$\frac{\partial v_z}{\partial z} + \underbrace{v_r \frac{\partial v_z}{\partial r}}_{\Updownarrow} + v_z \frac{\partial v_z}{\partial z} = -\frac{1}{\rho}\frac{\partial p}{\partial z} + \frac{\eta}{\rho}\left(\frac{\partial^2 v_z}{\partial r^2} + \frac{1}{r}\frac{\partial v_z}{\partial r} + \frac{\partial^2 v_z}{\partial r^2}\right)$$

$$\frac{\partial}{\partial r}(v_r v_z) - \underbrace{v_z \frac{\partial v_r}{\partial r}}_{\Updownarrow}$$

$$v_z \frac{\partial v_z}{\partial z} + \frac{v_r v_z}{r} \quad \text{using the continuity equation.}$$

The resulting equation is averaged over the cross section

$$\int_0^{2\pi}\int_0^R \left(\frac{\partial v_z}{\partial z} + \frac{\partial (v_z)^2}{\partial z} + \frac{1}{r}\frac{\partial}{\partial r}(r v_r v_z)\right) r dr d\vartheta$$

$$= \int_0^{2\pi}\int_0^R \left[-\frac{1}{\rho}\frac{\partial p}{\partial z} + \frac{\eta}{\rho}\frac{1}{r}\frac{\partial}{\partial r}\left(r\frac{\partial v_z}{\partial r}\right)\right] r\, dr\, d\vartheta.$$

After performing the integration, approximating

$$\int_0^{2\pi}\int_0^R \left(\frac{\partial (v_z)^2}{\partial z}\right) r\, dr\, d\vartheta$$

with $\partial/\partial z\left(Av^2\right)$ and utilizing the continuity equation, one obtains for the axial velocity v averaged over the cross section

$$\frac{\partial v}{\partial t} + v\frac{\partial v}{\partial z} + \frac{1}{\rho}\frac{\partial p}{\partial z} = f. \tag{3.34}$$

The friction term,

$$f = \int_0^{2\pi}\int_0^R \frac{\eta}{\rho}\frac{1}{r}\frac{\partial}{\partial r}\left(r\frac{\partial v_z}{\partial r}\right) r dr d\vartheta = \cdots \frac{2\pi R}{\rho}\left(\eta\frac{\partial v_z}{\partial r}\right) = \frac{2\pi R}{\rho}\tau_w.$$

Thereby τ_w denotes the skin friction at the wall, according to Newton's friction law (3.13). There are various ways (nontrivial, not worked out here)

how this term (which depends on the velocity profile) can be approximated. Furthermore, the term

$$\int_0^{2\pi}\int_0^{R}\left(\frac{1}{r}\frac{\partial}{\partial r}\left(rv_r v_z\right)\right) r\,dr\,d\vartheta$$

can be integrated and vanishes providing that there is no leakage through the wall.

A similar (straightforward) averaging scheme is used for the continuity equation which yields

$$\frac{\partial}{\partial z}\left(Av\right)+\frac{\partial A}{\partial t}=0. \tag{3.35}$$

Together with a constitutive equation for the wall $A\left(p\left(z,t\right),z\right)$ (which may include viscoelastic contributions) Eqs. (3.34) and (3.35) represent the hydraulic approximation.

This approximation yields good results if applied for arterial pulse propagation (Figs. 3.14, 3.15).

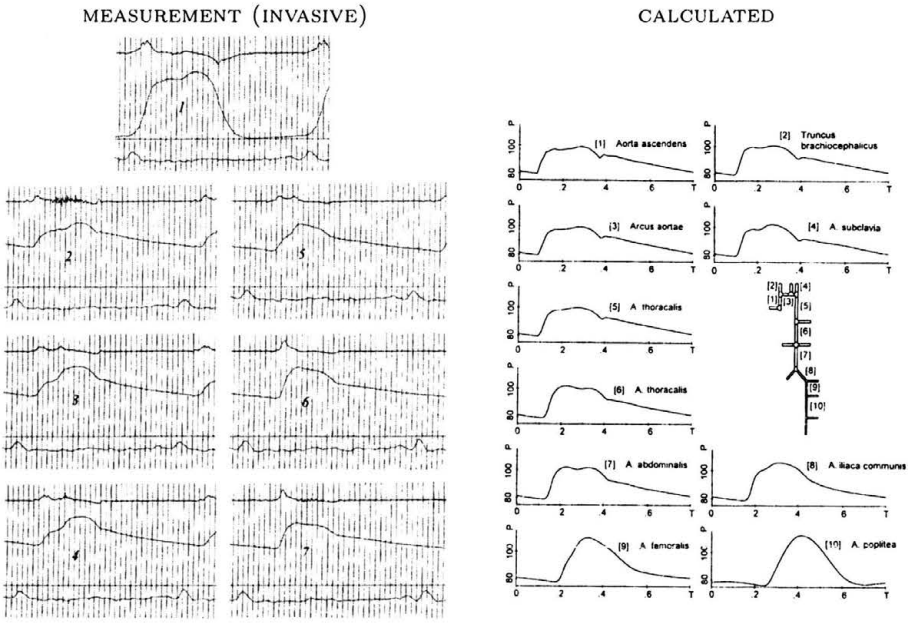

FIGURE 3.14. Pressure pulses in the arterial tree beginning at the heart and ending at the foot. Measurements (left) were made invasively, the calculations (right) were based on the hydraulic approximation.

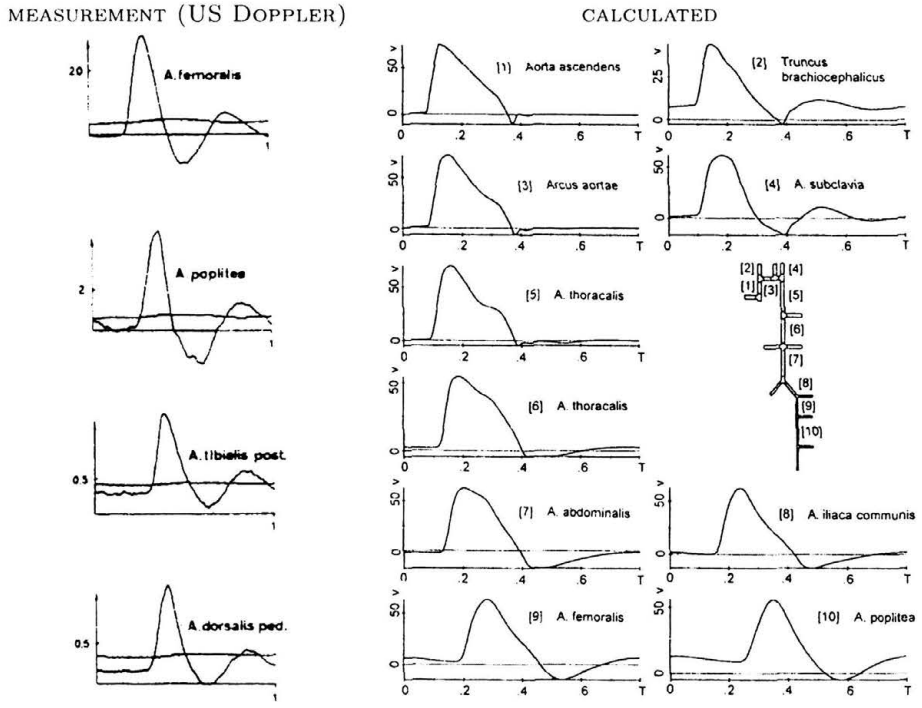

FIGURE 3.15. Flow pulses in the arterial tree beginning at the heart and ending at the foot. Measurements (left) were made noninvasively (ultrasound Doppler), the calculations (right) were based on the hydraulic approximation

3.6. Numerical Procedures

Most realistic problems in biomechanics cannot be solved analytically, accordingly, numerical solution procedures have to be chosen. For partial differential equations, three general methods have established themselves, two mostly applied within Euler representations, one within the framework of a Lagrange formulation.

When differential quotients are approximated by *Finite Difference Quotients*, the equations themselves are approximated. The resulting (in general large) set of linear algebraic equations is solved exactly (within machine precision).

The method of choice in biomechanics is the *Finite Element Method* (FEM). The method is particularly well suited for irregular geometries and nonlinear problems. Besides, a number of highly optimized commercial programs are available. In this method, the equations remain in their original

form, but the solution is piecewise approximated. Examples 3–6 show the application of FE models.

A significant drawback of FEM is associated with meshing, in particular, if the problem to be solved requires remeshing as is the case, e.g. for surgery simulation. A similar problem exists with finite difference methods. With the *Soft Particle Method*, originally introduced in astrophysics, remeshing can to some degree be avoided. The method consist of incorporating field quantities into radially symmetrical "smoothed particles" whose location and size are largely arbitrary, but have to allow for a suitable representation of the problem including all the desired details. Particles are created with the aid of a scalar function $W(\mathbf{r}, h)$ which is called the smoothing kernel with core radius h (finite support).

The function is radially symmetric and normalized,

$$\int_{\text{core area}} W(\mathbf{r}, h)\, d\mathbf{r} = 1.$$

Typical functions have an inverted bell-like form and are zero for $r > h$.

A field quantity A is interpolated from the particles as

$$A_{\mathrm{s}}(\mathbf{r}) = \sum_j m_j \frac{A_j}{\rho_j} W(\mathbf{r} - \mathbf{r}_j, h) \tag{3.36}$$

where

- j iterates over all particles
- m_j is the mass of a particle
- ρ_j the density
- $\mathbf{r}_j$ the position
- A_j the field quantity at $\mathbf{r}_j$.

The subscript "S" denotes a smoothed quantity. As is seen from (3.36), derivatives act only on W. For dynamic simulations, the interaction between particles in the form of force fields has to be modeled such that the physical behavior of the material (fluid, solid) is correctly approximated. Often, the equations are formulated and solved in Lagrange form.

References

1. R.N.L. NARASIMHAN, *Principles of Continuum Mechanics*, J.Wiley & Sons, 1993.

2. H. YAMADA, *Strength of Biological Materials*, Krieger Publ. Co, NY 1973.

Chapter 4

Diffusion and Osmosis

4.1. Diffusion

Biological tissues are generally of a multiphase nature, whereby water is the primary component: about 55%–70% of the volume of the human body consist of water. Accordingly, the transport of nutrients, oxygen, hormones, cytokines etc. from the location of uptake (intestine, lung) or production (glands, liver) to the cells of the various organs occurs in a water solution; likewise, waste products are brought to the excreting organs (kidney, liver, lung) through a water phase. Also intracellular transport is essentially fluid-based although transport by or along carrier or directing molecules is thereby dominant.

Driving mechanisms for transportation in biological systems are based on

- convection,
- diffusion,
- active transport by or along transport molecules,
- pinocytosis,
- transport by cells.

Convection and diffusion are passive in nature (with the exception of forced convection, see below) and can be described systematically by well known equations (Navier-Stokes equations in case of convection, Fick's law for diffusion, see below). In contrast, transport by carrier molecules and pinocytosis (vesicle transport through cells) involves active processes which are characterized by a great variety of different mechanisms most of which defy a "simple" mathematical description. Transportation by cells occurs,

e.g., in case of red blood cells which carry oxygen and CO_2 or with antigen-presenting leukocytes. Again, such transportation schemes cannot be modeled theoretically in a straightforward manner.

While the Navier-Stokes equations were treated in the last chapter, we turn our attention in the following to diffusion. Both convection and diffusion are of paramount importance for all aspects of physiological processes. While convection is driven by pressure gradients, diffusion is due to concentration gradients. Because of Brownian motion, more molecules in a homogeneous medium diffuse on the average from locations with a high concentration to locations where the concentration is lower than in the opposite direction. In general engineering practice, convection is thereby considered rapid and effective while diffusion is slow. In biology, however, this notion has to be applied with care because transport distances to be covered by convection and diffusion differ greatly.

Typical convection distances and times, e.g., in the systemic circulation are on the order of centimeters to meters and seconds to minutes, respectively. The intravascular volume (typically 5 liters of blood for an adult) circulates at rest once per minute because the cardiac output is around 5 l/min. (70 ml of blood times 70 beats per min.). There is substantial variability, however, in that in the case of highly perfused tissues (e.g. brain) typical circulation times are around 20 sec., while for bone and joints it is up to 15 min. The average flow velocity in the aorta is ca. 20 cm/sec. at rest with a peak of about 1.5 m/sec. Under conditions of heavy exercise, these values are markedly increased.

To obtain an approximate relation for typical diffusion times and distances, we consider a simple one-dimensional model. We start from an arbitrary distribution of a substance in a homogeneous solvent (Fig. 4.1). $N(x,t)$

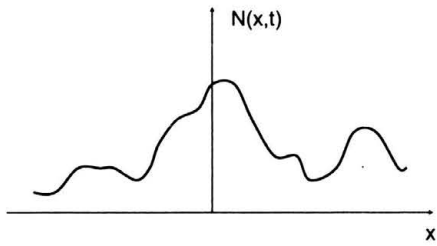

FIGURE 4.1. One-dimensional arbitrary (non-equilibrium) distribution of particles subjected to Brownian motion

denotes the concentration of the solute (number of particles per volume) at location x at time t. We assume, that the Brownian motion is translationally invariant, i.e., the probability that a particle moves from the location x to x' during the time interval ΔT due to Brownian motion depends on the one hand only on the distance $d = x' - x$ and is independent of x itself, and on the other hand on the time interval ΔT. Let this probability be denoted by $p_{\Delta T}(x' - x)$. It is furthermore symmetric, i.e., $p_{\Delta T}(x' - x) = p_{\Delta T}(-(x' - x))$ because the Brownian motion acts equally in both directions.

At time $t' = t + \Delta T$ the number of particles at location x' is

$$N(x', t + \Delta T) = \int_{-\infty}^{\infty} N(x, t) \cdot p_{\Delta T}(x' - x)\, dx.$$

After the transformation $X = x' - x$ we arrive at

$$N(x', t + \Delta T) = \int_{-\infty}^{\infty} N(x' - X, t) \cdot p_{\Delta T}(X)\, dX.$$

This relation is now subjected to a Taylor expansion

$$N(x', t) + \Delta T \left.\frac{\partial N}{\partial t}\right|_t + \ldots$$
$$= \int_{-\infty}^{\infty} \left(N(x', t) - X \left.\frac{\partial N(x, t)}{\partial x}\right|_{x=x'} + \frac{1}{2} X^2 \left.\frac{\partial^2 N(x, t)}{\partial x^2}\right|_{x=x'} - \ldots \right) p_{\Delta T}(X) dX. \tag{4.1}$$

Because of the symmetry property,

$$\int_{-\infty}^{\infty} X p_{\Delta T}(X) dX = 0$$

such that the second term on the right hand side of Eq. (4.1) disappears. Furthermore, since $p_{\Delta T}$ is a probability,

$$\int_{-\infty}^{\infty} p_{\Delta T}(X) dX = 1.$$

Upon discarding higher order terms and retaining only the leading terms, Eq. (4.1) reads

$$\frac{\partial N}{\partial t} = \frac{1}{2\Delta T}\frac{\partial^2 N}{\partial x^2}\int_{-\infty}^{\infty} X^2 p_{\Delta T}(X)dX = \frac{1}{2\Delta T}\frac{\partial^2 N}{\partial x^2}\langle X^2\rangle \tag{4.2}$$

whereby $\langle X^2\rangle$ denotes the average of the squared displacement which a particle undergoes during ΔT. Eq. (4.2) is known as Fick's diffusion equation

$$\frac{\partial N}{\partial t} = D\frac{\partial^2 N}{\partial x^2} \tag{4.3}$$

with the diffusion constant

$$D = \frac{\langle X^2\rangle}{2\Delta T} \tag{4.4}$$

Note: In the derivation of eq. (4.3) it was implicitly assumed that the frequency of collisions associated with the Brownian motion is sufficiently high such that there are numerous collisions during the time interval ΔT and a true average is reached.

From a known diffusion constant typical time intervals necessary for diffusive transport over a distance d can therefore be estimated using the relation (4.4). Table 4.1 has been derived from tabulated diffusion constants for free diffusion in water.

TABLE 4.1. Typical diffusion constants D of molecules (mol. weight 40, 1 000 and 20 000, respectively) in water. Representative time intervals T which are necessary for molecules to diffuse on the average over a distance d were estimated from Eq. (4.4).

D [m^2/s]	$d = \sqrt{\langle X^2\rangle}$ [μm]	T [s]	mol. weight
10^{-9}	10	0.1	40
10^{-9}	100	10	
10^{-10}	10	1	1 000
10^{-10}	100	100	
10^{-11}	10	10	20 000
10^{-11}	100	1 000	

It is seen that for short distances, diffusion may be rapid. In biological tissues, diffusion distances are determined by the density of capillaries which

varies greatly from tissue to tissue. For well perfused tissues, capillary-to-capillary distances are on the order of 20 μm to 100 μm, accordingly, diffusion is sufficiently effective to keep homeostasis.

Different conditions are encountered in tissues which are weakly perfused, in particular in compact bone where the bone matrix is essentially impermeable for fluids. Haversian or lamellar (compact) bone is composed of cylindrically shaped osteons which have a diameter of about 100 μm–400 μm. Each osteon is perfused by a central capillary located in the Haversian canal. The bone cells (osteocytes) are distributed throughout the shell-like solid structure of the osteons and reside in openings within the bone matrix called lacunae (diameter a few μm). The lacunae, in turn, are connected by a dense net of canaliculi, through which the metabolic traffic of osteocytes occurs (Fig. 4.2). Since the canaliculi have diameters of less than about 400 nm and osteon-osteon distances are around 30 μm typically, diffusion is by far insufficient to provide adequate transport capacity. This can be seen from a simple one-dimensional model (Fig. 4.3).

Given the boundary conditions for the concentration $c(z,t)$ of a sample substance (z denotes the axial coordinate along the one-dimensional conduit) which is introduced at time zero and then kept constant at the inlet of the tube,

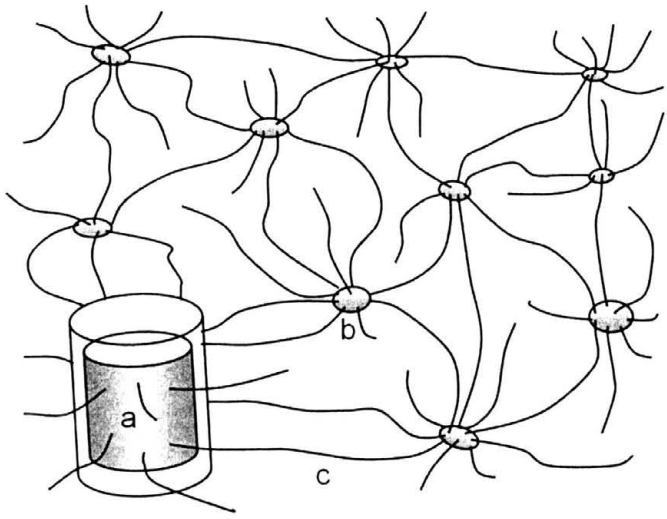

FIGURE 4.2. Schematic (not scaled) view of compact bone; (a) Haversian canal with central capillary; (b) lacuna, containing osteocyte; (c) canalicular network

$$t < 0 : c(z,t) = 0,$$
$$t > 0 : c(z = 0, t) = c_0, \quad \text{(constant)}$$
$$t > 0 : c(z = \infty, t) = 0,$$

the diffusion equation,

$$\frac{\partial^2 c}{\partial z^2} = \frac{1}{D}\frac{\partial c}{\partial t}$$

is best subjected to a Laplace transform

$$\frac{\partial^2 \tilde{c}}{\partial z^2} = \frac{s}{D}\tilde{c}.$$

Here s denotes the variable associated with the Laplace transform and $\tilde{c}$ is the Laplace transform of c. The boundary conditions read

$$\tilde{c}\,(s, z = 0) = \frac{c_0}{s},$$
$$\tilde{c}\,(s, z = \infty) = 0,$$

and the solution (after performing the inverse transform) is obtained as

$$c(z,t) = c_0 \operatorname{erfc}\left(\frac{z}{2\sqrt{Dt}}\right) \tag{4.5}$$

where $\operatorname{erfc}(x) = 1 - \operatorname{erf}(x)$. The flow per unit area, $Q = -D\,dc/dz$ can be calculated from (4.5) as

$$Q = c_0 \left(\frac{D}{\pi t}\right) \mathrm{e}^{-\left(\frac{z}{2\sqrt{Dt}}\right)^2}$$

using the differentiation properties of the error function. The exponential factor for $z = 10\,\mu\text{m}$, $D = 10^{-8}\,\text{cm}^2/\text{s}$, $t = 1\,\text{s}$, say, is close to zero. It can be

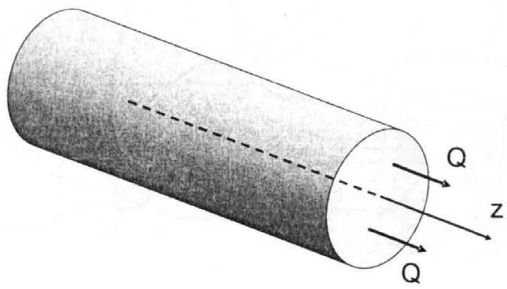

FIGURE 4.3. One-dimensional diffusive flow Q; z: axial coordinate of model canaliculus

shown (Example VI) that bone perfusion is primarily due to forced convection and not diffusion: As a result of the loading environment to which bones are exposed during normal daily activity (walking, working, etc.) the bone matrix undergoes small deformations. Since the fluid contained in the lacunocanalicular system is nearly incompressible, load-induced pressure gradients build up which set the fluids in motion. Load-induced fluid flow or forced convection has been found to be an extremely powerful and affective transport mechanism.

4.2. Osmosis

A particularly important effect associated with diffusion occurs in systems which are subdivided into compartments separated by semipermeable membranes, i.e. barriers which are permeable selectively for certain molecules only. While the solvent, e.g., water can diffuse freely between the compartments through the diffusive barrier, the solute cannot, because, e.g., the molecules are too big to penetrate the membrane. Whenever concentration differences exist across the barrier, a pressure difference develops in thermodynamic equilibrium, called osmotic pressure. It is found that osmosis is an important driving mechanism in many biological transport processes. In practice, and analysed in the following, an osmotic pressure is observed whenever a semipermeable membrane separates two fluid spaces containing mixtures with different concentrations, whereby the membrane is permeable for the solvent and impermeable for the solute.

A short derivation of van't Hoff's law, which describes the simplest form of osmotic pressure is given in the following (a more general treatment can be found in [1] or [2]). Van't Hoff's law is valid for diluted solutions and small molecules.

We consider first a homogeneous system consisting of one substance. According to the second law of thermodynamics, the change of entropy, dS, of such a system when subjected to an infinitesimal state change, can be written as

$$dS \geq \sum_k X_k dx_k. \tag{4.6}$$

X_k thereby denote "intensive" quantities (independent of the amount of material such as the temperature T, or the pressure p) while the associated x_k are "extensive" quantities (dependent on the amount of material such as the

internal energy, U, or the volume, V). The equality holds for reversible processes, whereas in case of irreversible state changes, the entropy increases by an additional amount.

If the system can be described by the aforementioned four quantities, Eq. (4.6) reads

$$dS \geq \frac{1}{T} dU + \frac{p}{T} dV. \tag{4.7}$$

In this equation, the entropy appears as a function of the extensive quantities U, V as independent variables. Since we will be considering transport processes, it is more useful to have a representation with intensive quantities as independent variables. This is reached by the following transformation which introduces the Gibbs potential, G,

$$G = U + pV - TS. \tag{4.8}$$

Upon calculating the total differential, dG, and using (4.7), one obtains

$$dG(p, T) \leq -SdT + Vdp \tag{4.9}$$

which exhibits the desired form and from which follows, among other,

$$\left.\frac{\partial G}{\partial p}\right|_T = V. \tag{4.10}$$

We turn our attention now to homogeneous mixtures of various substances, i, $i = 1, \ldots, k$. The numbers of moles of each substance in the mixture, n_i, thereby serve as additional extensive quantities. The associated intensive quantities, μ_i, are denoted as chemical potential of each substance, such that

$$dG(p, T, n_i) \leq -SdT + Vdp + \sum_k \mu_i n_i. \tag{4.11}$$

It is furthermore useful to relate all intensive quantities for each substance to the number of moles, i.e.,

$$v_i = \left.\frac{\partial V}{\partial n_i}\right|_{p,T,n_j}, \quad s_i = \left.\frac{\partial S}{\partial n_i}\right|_{p,T,n_j}, \quad j \neq i \tag{4.12}$$

such that (4.11) can be written as

$$dG \leq \sum_k \left[(-s_i dT + v_i dp)\, n_i + \mu_i dn_i\right]. \tag{4.13}$$

Equation (4.13) shows that the chemical potential, μ_i, has the meaning of the molar Gibbs potential, i.e.,

$$\mu_i = \left.\frac{\partial G}{\partial n_i}\right|_{p,T,n_j} \quad \text{and} \quad G = \sum_k \mu_i n_i. \tag{4.14}$$

For what follows, we will make use of the pressure dependence of the chemical potential of an ideal gas. From

$$\left.\frac{\partial \mu_i}{\partial p}\right|_T = v_i \tag{4.15}$$

one obtains

$$\mu_i - \mu_i^0(T)\Big|_{p_0} = \int_{p_0}^{p_i} v_i dp\Big|_{T=\text{const}} = \int_{p_0}^{p_i} \frac{RT}{p} dp = RT \log\left(\frac{p_i}{p_0}\right) \tag{4.16}$$

where the ideal gas law, $p_i v_i = RT$, has been applied; p_0 denotes some arbitrary reference state, while p_i is the partial pressure of the component i in the mixture. According to Dalton's law, for ideal gases, the following relations hold.

$$p = \sum_k p_i \quad \text{and} \quad \frac{p_i}{p} = \frac{n_i}{n}, \quad n = \sum_k n_i. \tag{4.17}$$

Since we consider liquid mixtures we need the pressure dependence of the chemical potential of a liquid. This is obtained from the equilibrium between the liquid and associated vapor phase of a fluid. When dn moles of the liquid phase evaporate into the vapor phase, the Gibbs potential changes according to

$$dG = (\mu^{\text{v}} - \mu^{\text{li}})dn \tag{4.18}$$

whereby μ^{v} denotes the chemical potential of the vapor and μ^{li} the chemical potential of the liquid phase, respectively. The Gibbs potential changes spontaneously in an irreversible fashion until thermodynamic equilibrium is reached, i.e., $dG = 0$. This implies that the chemical potentials are equal, i.e.,

$$\mu_i^{\text{li}} = \mu_i^{\text{v}}\Big|_{p_0} + RT \log\left(\frac{p_i}{p_0}\right) \tag{4.19}$$

if it is assumed that the vapor obeys the ideal gas relation.

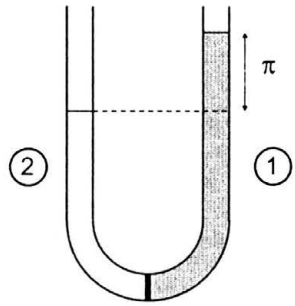

FIGURE 4.4. U-shaped tube with two compartments separated by a semipermeable membrane S. (1) pure solvent; (2) solution, π: osmotic pressure difference

Upon introducing the total pressure p, we obtain

$$\begin{aligned}\mu_i^{\mathrm{li}} &= \mu_i^v\Big|_{p_0} + RT\,(\log p_i - \log p_0 + \log p - \log p) \\ &= \mu_i^v\Big|_{p_0} + RT\left(\log\left(\frac{p_i}{p}\right) + RT\left(\frac{p}{p_0}\right)\right) = \mu_i^{\mathrm{li}}\Big|_p + RT\log\left(\frac{p_i}{p}\right). \quad (4.20)\end{aligned}$$

Following Dalton's law (4.17), finally one obtains the relation

$$\mu^{\mathrm{li}} = \mu^{\mathrm{li}}\Big|_{n_i=n} + RT\log\left(\frac{n_i}{n}\right). \quad (4.21)$$

After these preparatory derivations, we look at the system shown in Fig. 4.4. It consists of a U-shaped tube which is separated into two halves by a semipermeable membrane at the bottom. The tube is filled with a diluted solution and the membrane is permeable for the solvent but impermeable for the solute. The one side (side 1) of the tube contains a solution consisting of $n_{\mathrm{so}}^{(1)}$ moles of solute in $n_{\mathrm{ls}}^{(1)}$ moles of solvent ($n^{(1)} = n_{\mathrm{so}}^{(1)} + n_{\mathrm{ls}}^{(1)}$), while on the other (side 2) there is only solvent. It is empirically observed that the pressure on side 1 is higher by an amount, π, called osmotic pressure, than on side 2.

At equilibrium, the chemical potential of the solvent is the same on both sides of the membrane, $\mu_{\mathrm{ls}}^{(1)}$, $\mu_{\mathrm{ls}}^{(2)}$, respectively, because otherwise fluid is exchanged until the Gibbs potential reaches a minimum (in an analogous process as is formulated in Eq. (4.17)):

$$\mu_{\mathrm{ls\ (pure\ solvent)}}^{(2)}(p) = \mu_{\mathrm{ls\ (solution)}}^{(1)}\left(\frac{n_{\mathrm{ls}}^{(1)}}{n^{(1)}}, p + \pi\right). \quad (4.22)$$

Utilizing Eq. (4.20) and (4.15) yields

$$\mu_{\mathrm{ls}}^{(2)}(p) = \mu_{\mathrm{ls}}^{(1)}(p+\pi) + RT \log\left(\frac{n_{\mathrm{ls}}^{(1)}}{n^{(1)}}\right) = \mu_{\mathrm{ls}}^{(1)}(p) + \int_{p}^{p+\pi} v\,dp + RT \log\left(\frac{n_{\mathrm{ls}}^{(1)}}{n^{(1)}}\right). \tag{4.23}$$

Since the molar volume v, of a liquid is approximately constant under the pressures of interest here and $\mu_{\mathrm{ls}}^{(1)}(p)$ and $\mu_{\mathrm{ls}}^{(2)}(p)$ are the same, the integral in Eq. (4.23) equals $v\pi$. Accordingly

$$v\pi = -RT \log\left(\frac{n_{\mathrm{ls}}^{(1)}}{n^{(1)}}\right) = -RT \log\left(1 - \frac{n_{\mathrm{so}}^{(1)}}{n^{(1)}}\right) \approx RT\left(\frac{n_{\mathrm{so}}^{(1)}}{n^{(1)}}\right)$$

or, since in case of a diluted solution, the total volume $V \approx vn^{(1)}$,

$$\pi = RT\left(\frac{n_{\mathrm{so}}^{(1)}}{V}\right) = RT\left(\frac{c}{M_{\mathrm{so}}}\right) \quad \text{(van't Hoff's law)}. \tag{4.24}$$

Here M_{so} denotes the molecular weight of the solutes, and c the concentration,

$$c = \left(\frac{n_{\mathrm{so}}^{(1)} M_{\mathrm{so}}}{V}\right).$$

Van't Hoff's law in the form (4.24) holds for diluted solutions and solutes with small molecular weights. For increasing M_s, π is seen to decrease. Yet, the ideal gas approximation is not valid in case of large molecules because in such substances the intermolecular potentials cannot be disregarded (in an ideal gas, there are no interactions between the particles other than collisions causing equilibrium; there are in particular no intermolecular potentials).

Osmosis still occurs in case of solutions involving large molecules (proteins), but its effect cannot be derived in a straightforward manner. A method called virial expansion which is based on a correlation analysis (second order correlations relate to pair-wise interaction of molecules, the third order to triple interactions, etc.) allows to expand the osmotic or oncotic pressure (sometimes called "oncotic" in order to distinguish it from the previous form) according to

$$\pi = RT\left(\frac{c}{M_s} + A_2 c^2 + A_3 c^3 + \ldots\right). \tag{4.25}$$

The A_i are called virial coefficients.

In the case of blood, where water is the solvent, the osmotic pressure caused by the electrolytes in solution (Na^+, Ca^{++}, Cl^-, etc., ca. 1 g/100 ml plasma) is about 750 kPa. This enormous pressure does not occur in the human circulation, however, because the capillaries are generally permeable for all molecules of this (small, see below) size (the permeability of larger blood vessels is such that osmotic pressures do not develop across the vessel wall). An important exception consists of the vasculature of the central nervous system where capillaries are largely impermeable for all molecules (blood-brain barrier; exchange of substances across this barrier is essentially based on active transport processes).

The blood contains also large molecules, viz., the plasma proteins (molecular weight from some 10 000 up to 300 000 Dalton). As a rule of thumb, "small" and "large" refers to a molecular weight of less than or more than 5 000 Dalton. Capillary walls, in particular on the arterial side, including the endothelial glycocalix are to a great extent impermeable for large molecules, i.e. for proteins. Accordingly, an oncotic pressure develops which for a plasma protein concentration of about 7.5 g/100 ml plasma is around 3.3 kPa. This is the basis of Starling's hypothesis which represents a simple model for the description of capillary exchange in tissues other than the CNS.

Starling's formula for the fluid flow per unit area through the capillary wall J is usually given as

$$J = p_c \, (\Delta p - \varepsilon \Delta \pi) \tag{4.26}$$

whereby p_c is a parameter characterizing the permeability of the wall, Δp the hydrostatic pressure difference (difference between the fluid pressure inside the capillary and the interstitial space), and $\Delta \pi$ the oncotic pressure difference (difference due to the different plasma protein concentration in the intra- and extravascular space); ε is a correction factor ("reflection coefficient") which takes into account effects such as the small leakage of proteins through the capillary wall, mostly on the venous side due to large openings, called "fenestrations".

Starling's hypothesis has been substantiated qualitatively in many tissues mostly in animal experiments. Nevertheless, the microcirculation is different from tissue to tissue and depends largely on the local physiological characteristics. In addition to the passive flow approximated by Eq. (4.26), there are numerous active transport processes.

References

1. P.W. ATKINS and J. DE PAULA, *Physical Chemistry*, Oxford University Press, 2001

2. L.D. LANDAU and E.M. LIFSHITZ, *A Course of Theoretical Physics*, Vol. 5, Butterworth-Heinemann, 4th ed., 1980

Examples

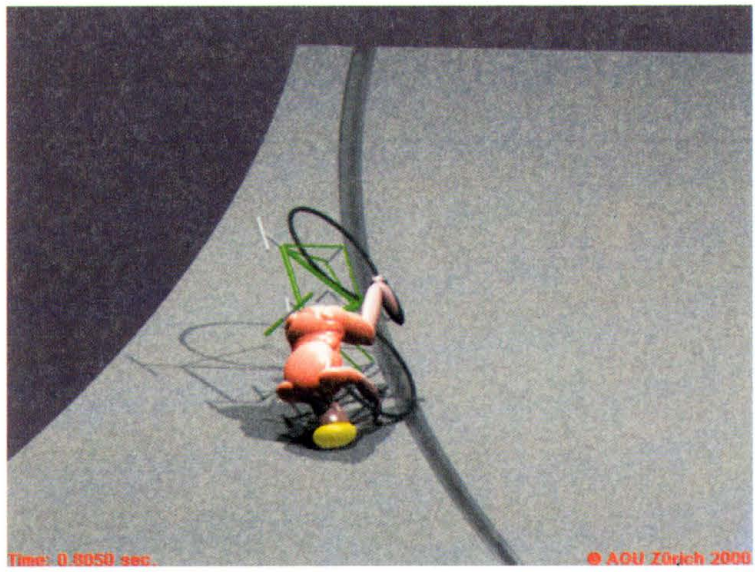

EXAMPLE I. Cyclist trapped in tram rail. The cyclist as well as the bicycle were modeled as systems of rigid bodies. Contacts were approximated with the aid of a mutual force-penetration algorithm.

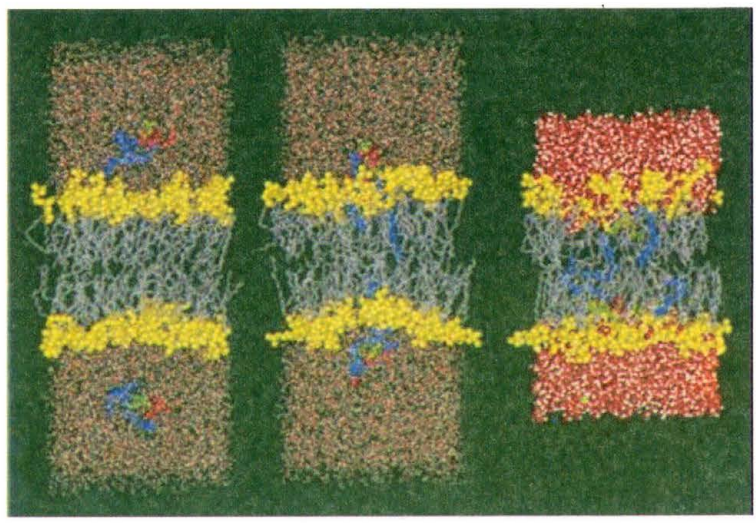

EXAMPLE II. Snapshots of the insertion of a peptide (red-blue-green) into a biological membrane (yellow-gray), after 0.25 nsec. (left), 0.35 nsec (middle) and 0.42 nsec (right). Above and below the membrane are numerous water molecules. For details the reader is referred to A.A. Gorfe, R. Pellarin, A. Caflisch, *Membrane localization and flexibility of a lipidated ras peptide studied by molecular dynamics simulations*, J. Am. Chem. Soc. **126**: 15277, 2004. Used with permission.

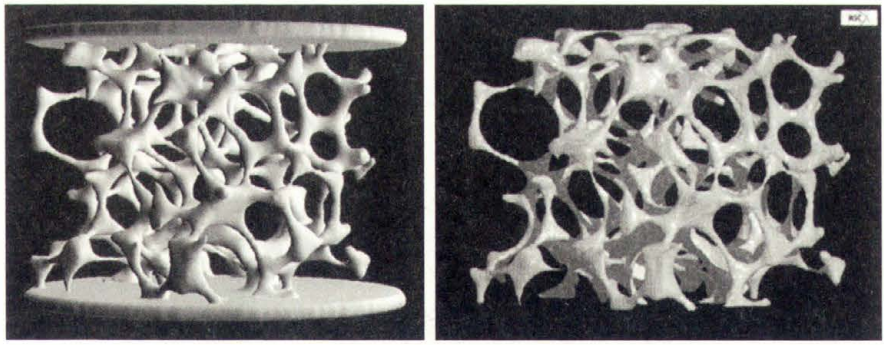

IGFA/Experimental FEM/Simulation

EXAMPLE III. Image guided failure analysis: deformation of a trabecular bone sample under compressive load as recorded by μCT (left). Corresponding mathematical model, FE simulation (right). (Courtesy: R. Müller, ETH Zurich)

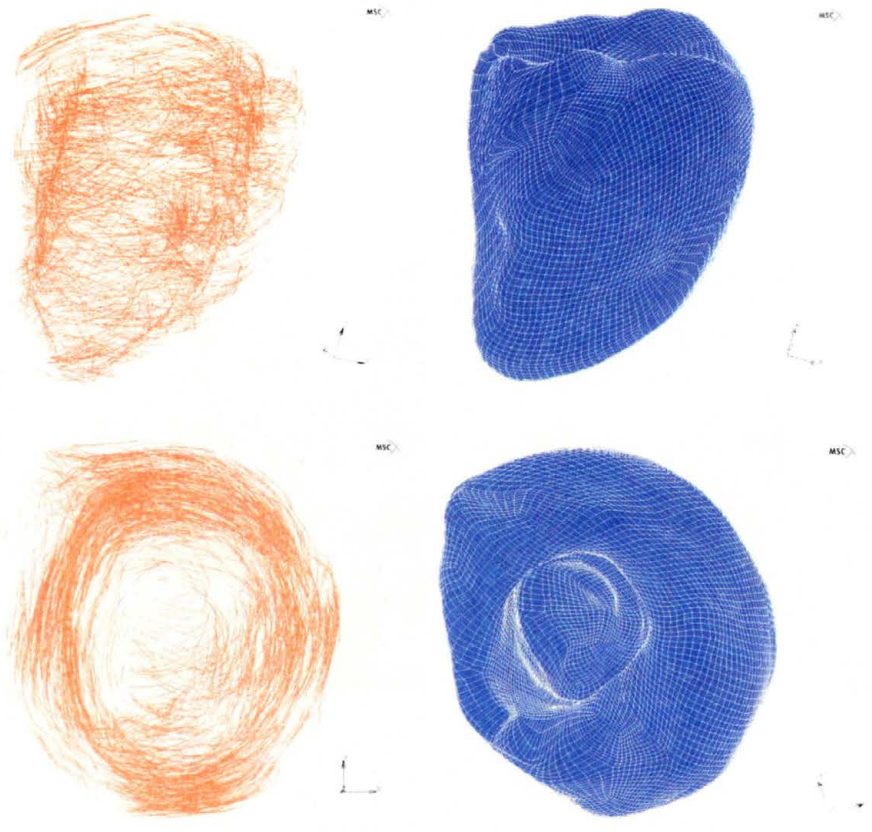

EXAMPLE IV. Anisotropic heart model: Fiber architecture as determined from fiber peeling (left), corresponding FE model (right).

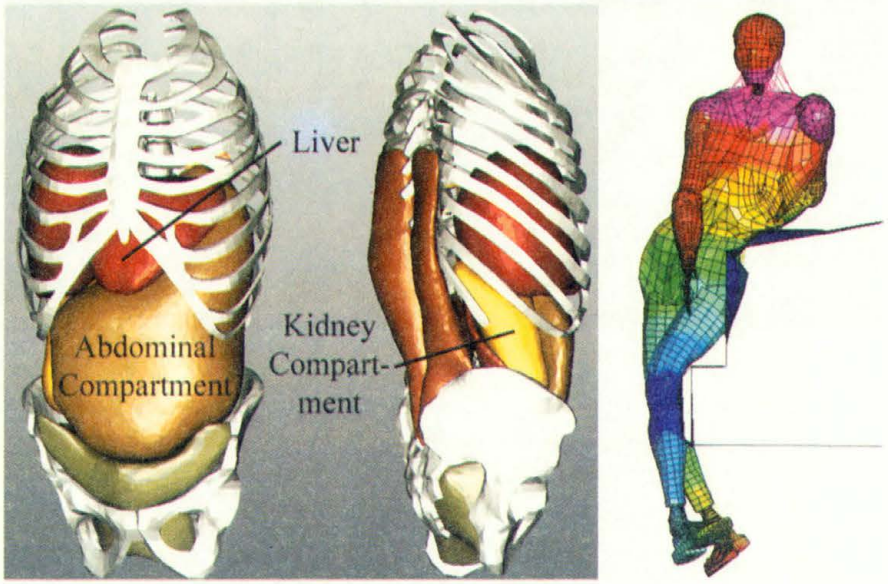

EXAMPLE V. FE model for injury analysis: thorax and abdomen including internal organs (left) and whole-body pedestrian impact model (right).

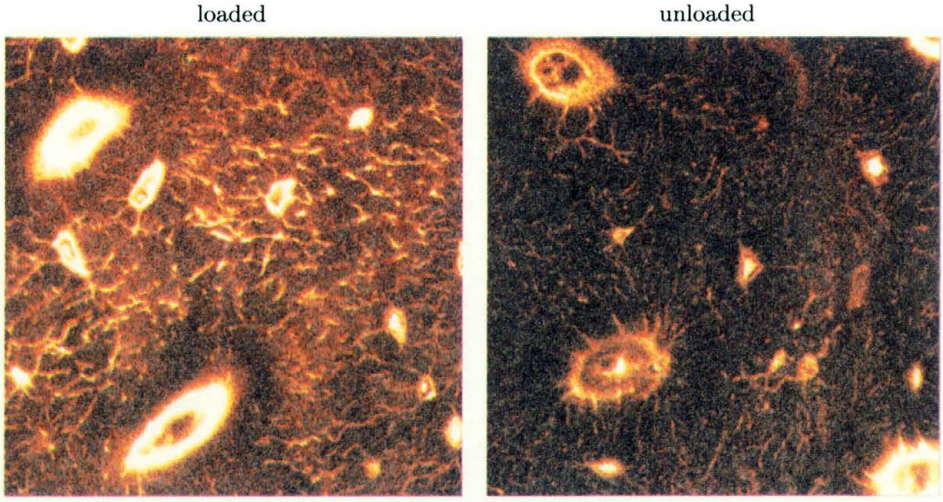

EXAMPLE VI. Forced convection in compact rat bone: an anesthetized rat was perfused systemically for 5 minutes with procion red (inert fluorescent dye, molecular weight 200 Dalton). The lower leg was subsequently subjected to cyclic loading representative for walking (microscopic preparation of bone sample, left), while the contralateral side remained unloaded (right). The effect of load-induced perfusion is seen from the intensity of fluorescence (magnification $\times 1000$).

Already appeared in the ABIOMED *Lecture Notes* series:

1. J. MIZRAHI, *Muscle/Bone Interactions in the Musculo-Skeletal System*
2. A. NOWICKI and J. LITNIEWSKI (Eds.), *Proceedings of the Workshop on Ultrasound in Biomeasurements, Diagnostics and Therapy*
3. J. PIEKARSKI (Ed.), *Tissue Remodelling*
4. S. SIDEMAN, *Insight into the Heart: Cardiac Energetics*
5. T. LEKSZYCKI and P. MAŁDYK (Eds.), *Biomaterials in Orthopaedic Practice*
6. T.A. KOWALEWSKI (Ed.), *Blood Flow Modelling and Diagnostics*

INSTITUTE OF FUNDAMENTAL TECHNOLOGICAL RESEARCH
publishes the following periodicals:

ARCHIVES OF MECHANICS — bimonthly (in English)
ARCHIVES OF ACOUSTICS — quarterly (in English)
ARCHIVES OF CIVIL ENGINEERING — quarterly (in English)
ENGINEERING TRANSACTIONS — quarterly (in English)
COMPUTER ASSISTED MECHANICS AND ENGINEERING SCIENCES — quarterly (in English)
JOURNAL OF TECHNICAL PHYSICS — quarterly (in English)

Subscription orders for all journals published by IFTR may be sent directly to:

Editorial Office
Institute of Fundamental Technological Research
Świętokrzyska 21
00-049 Warsaw, POLAND